Marine and Petroleum Geology 110 (2019) 138–161

Contents lists available at ScienceDirect

Marine and Petroleum Geology

journal homepage: www.elsevier.com/locate/marpetgeo

Research paper

Determining continuous basins across conjugate margins: The East Orphan, Porcupine, and Galicia Interior basins of the southern North Atlantic Ocean

Larry Sandoval[a,*], J. Kim Welford[a], Heide MacMahon[a], Alexander L. Peace[a,b]

[a] Department of Earth Sciences, Memorial University of Newfoundland, St. John's, Newfoundland, A1B 3X5, Canada
[b] School of Geography and Earth Sciences, McMaster University, Hamilton, Ontario, L8S 4K1, Canada

ARTICLE INFO

Keywords:
Conjugate margins
Crustal architecture
Kinematic evolution
Rifted margins
Structural restoration
Crustal thinning
Rifting
Hyperextension
Newfoundland
Ireland
Iberia
Petroleum geology

ABSTRACT

The East Orphan, Porcupine, and Galicia Interior basins are several of the most promising basins for hydrocarbon exploration along the rifted continental margins of the southern North Atlantic Ocean. Despite having formed at similar geological times, the basins exhibit fundamental differences in symmetry, crustal thickness, sedimentary cover thickness, and amount of extension. Interpretation of seismic reflection and well data was integrated with published 3D grids of depth-to-basement and Moho proxy depth to interpret and restore select seismic reflection lines. Publicly available kinematic evolution models were also integrated to evaluate and compare the restored seismic reflection lines in a more global regional context.

Interpretation of five seismo-stratigraphic units and three tectonostratigraphic megasequences along the East Orphan, Porcupine, and Galicia Interior basins reveals similar seismic character for each unit and comparable tectonic history. The structural restoration of the selected lines indicates that evolution, sedimentary cover thickness, faulting style, crustal structure, and kinematic evolution of the East Orphan and Porcupine basins differ significantly. A variable and asymmetrical crustal structure is found in the East Orphan Basin contrasting with the elongated and symmetric Porcupine and Galicia Interior basins. Rift domain maps of the three basins reveal that they are each underlain by hyperextended crust, with possible exhumed mantle in the centre of the Porcupine Basin.

Based on a holistic analysis of the results obtained, the linkage between the East Orphan and the Porcupine basins seems implausible, but rather a contemporaneous relationship is interpreted. Moreover, a potential connection between the Galicia Interior Basin and the Porcupine Basin during the Early to Late Jurassic is proposed. Such scenarios imply an oblique and synchronous rifting evolution around the Bay of Biscay triple junction of the southern North Atlantic.

1. Introduction

The East Orphan Basin, offshore Newfoundland, the Porcupine Basin, offshore Ireland, and the Galicia Interior Basin, offshore Iberia, represent three key basins along the rifted continental margins of the southern North Atlantic Ocean with promising hydrocarbon potential (Fig. 1). Considering these three basins together is crucial for understanding the evolution of the triple junction around which the southern North Atlantic Ocean opened.

Since the 1960s and 1970s these margins have been the focus of numerous studies (e.g., Department of Mines and Energy, 2000; Groupe Galice, 1979; Shannon et al., 2001). Previous authors have interpreted differences in the numbers and timing of rift phases (Enachescu et al., 2005; Gouiza et al., 2017; Norton, 2002; Shannon et al., 2007; Shannon and Naylor, 1998; Sibuet et al., 2007; Skogseid, 2010; Williams et al., 1999) and the style of rifting (Chian et al., 2001; Gouiza et al., 2017; Krawczyk et al., 1996; Lau et al., 2015; Murillas et al., 1990; Pérez-Gussinyé et al., 2003; Reston et al., 2004; Welford et al., 2012) along the Newfoundland, Irish Atlantic, and Iberian margins. However, in general, two main rifting phases occurred during the Late Triassic-Early Jurassic and Late Jurassic to Early Cretaceous, which affected the East Orphan, Porcupine, and Galicia Interior basins. As a result of the rifting episodes, several rift branches were simultaneously developed along the three margins. Most of the previous studies have been based on seismic interpretation, gravity inversion, and/or refraction data modelling and focused on only one or two of the margins (e.g., East Orphan and/or Porcupine basins). Rigid kinematic plate reconstructions have also resulted in disagreements about the connectivity of these basins during

* Corresponding author.
E-mail addresses: lsandoval@mun.ca (L. Sandoval), kwelford@mun.ca (J.K. Welford), hmacmahon@mun.ca (H. MacMahon), alpeace@mun.ca (A.L. Peace).

https://doi.org/10.1016/j.marpetgeo.2019.06.047
Received 20 February 2019; Received in revised form 21 June 2019; Accepted 26 June 2019
Available online 29 June 2019
0264-8172/

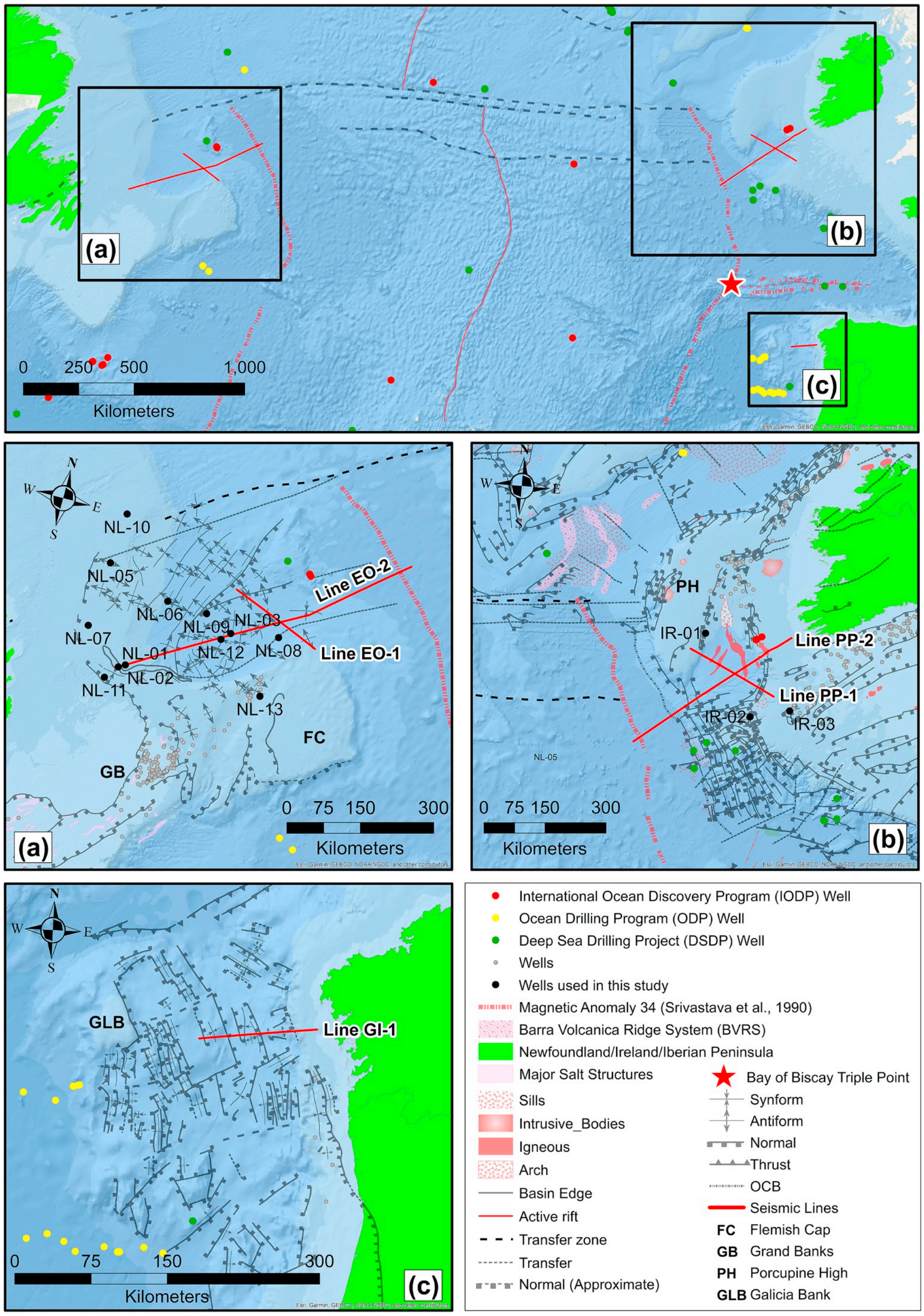

Fig. 1. Location of the study area. (a) Newfoundland margin. (b) Irish margin. (c) Galicia margin. Structural features extracted from Edwards et al. (2003) and Sibuet et al. (2007) for the Newfoundland margin, Naylor et al. (2002) for the Irish margin, Murillas et al. (1990) for the Galicia margin, and Bouysse and coll (2014) and Srivastava et al. (1990) for the southern North Atlantic.

rifting (Fig. 2), although many suggest a link between the East Orphan and Porcupine basins (e.g., Louden et al., 2004; Matthews et al., 2016; Seton et al., 2012; Skogseid, 2010). These often-conflicting theories illustrate the complexity of these conjugate margins.

Integration of geophysical and geological data provides a general template for enhancing our understanding of the tectonic evolution of complex basins (e.g., Decarlis et al., 2015; Peace et al., 2018b; Tugend et al., 2014; Welford et al., 2012). Previous studies have interpreted hyperextended crust for the East Orphan, Porcupine, and Galicia Interior basins (Lundin and Doré, 2011; Welford et al., 2012). Using data from these three hyperextended basins and applying an integrated approach, we interpret and restore select seismic lines. We interpret crustal domains beneath each of the basins and we integrate them with the restored lines and kinematic evolution models. Here, we reconnect the conjugate margin basins that were possibly once linked and try to better understand their evolution, with particular emphasis placed on the analysis of the East Orphan and Porcupine basins due to their commonly accepted link in the published literature and their key role in the evolution of the southern North Atlantic Ocean.

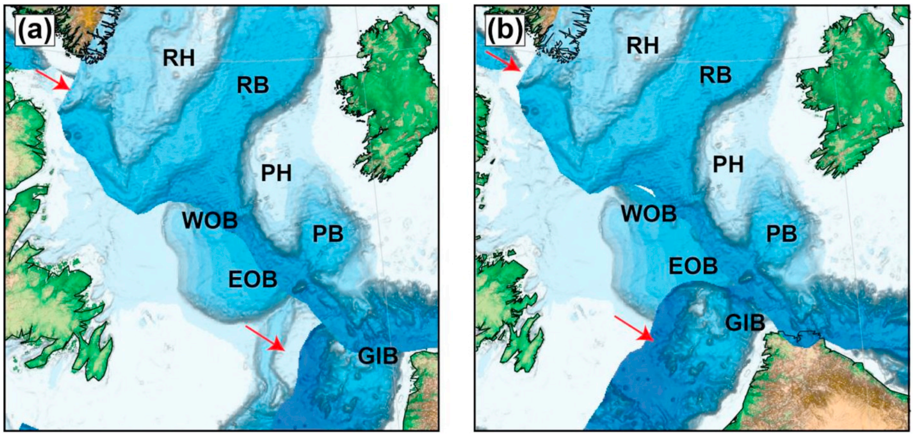

Fig. 2. Example of rigid plate reconstructions at the Early Jurassic (180 Ma). (a) Matthews et al. (2016), (b) Seton et al. (2012). Red arrows: zones of plate overlap due to the rigid plate assumption used in both models. RH: Rockall High. RB: Rockall Basin. PH: Porcupine High. PB: Porcupine Basin. WOB: West Orphan Basin. EOB: East Orphan Basin. GIB: Galicia Interior Basin. (For interpretation of the references to colour in this figure legend, the reader is referred to the Web version of this article.)

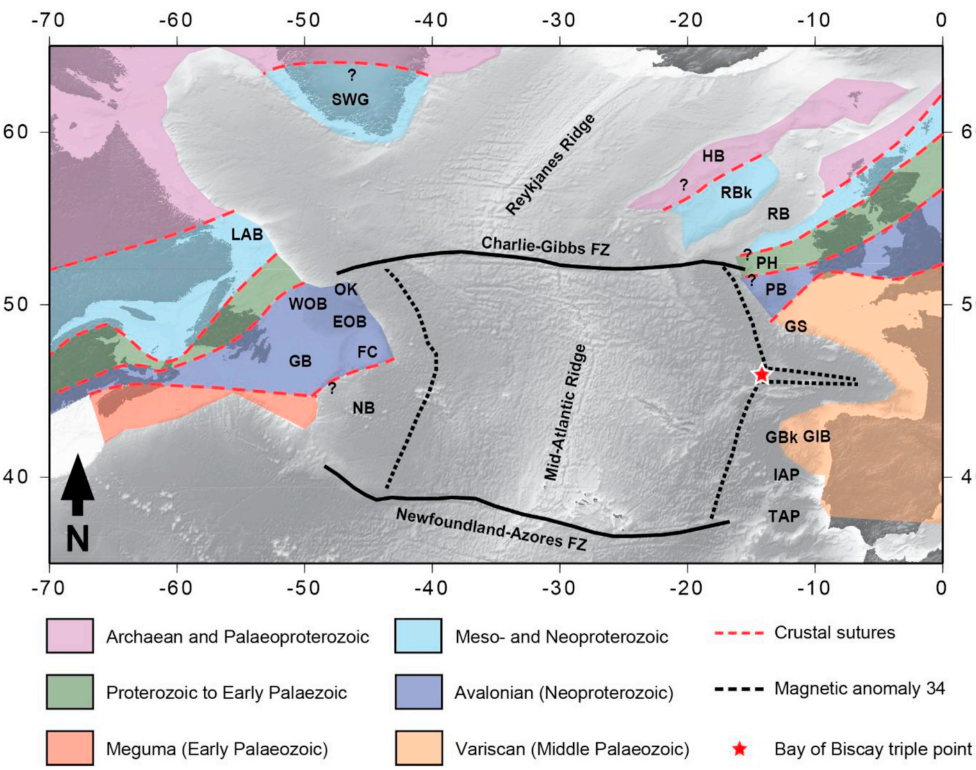

Fig. 3. Inferred basement affinity of continental crust of the North Atlantic (adapted from Tyrrell et al., 2007 and Welford et al., 2012). GB: Grand Banks. FC: Flemish Cap. NB: Newfoundland Basin. HB: Hatton Bank. RBk: Rockall Bank. RB: Rockall Basin. PH: Porcupine High. PB: Porcupine Basin. GS: Goban Spur. GBk: Galicia Bank. GIB: Galicia Interior Basin. IAP: Iberia Abyssal Plain. OK: Orphan Knoll. TAP: Tagus Abyssal Plain. LAB: Labrador margin. SWG-Southwest Greenland margin. FZ: fracture zone.

2. Tectonic setting

The current tectonic framework comprising Atlantic Canada, Western Ireland, and the Iberian Peninsula (Fig. 3), was established with the three-way continental collision between Baltica, Avalonia, and Laurentia (Domeier, 2016; Sibuet and Collette, 1991), which followed multiple ocean opening-closing cycles (Thomas, 2006; Wilson, 1966). These cycles included the formation of the Uranus Ocean in the Neoproterozoic and its closure during the Grenville Orogeny (1300-950 Ma), followed by the development of the Iapetus Ocean during the Late Ediacaran/Early Cambrian, which closed during the Appalachian Orogeny (600-300 Ma), the creation of the Rheic Ocean during the Early Ordovician, and finally the suturing together of Pangaea (Domeier, 2016; Frizon De Lamotte et al., 2015; Harland and Gayer, 1972; Murphy et al., 2010; Murphy and Nance, 2008; Nance et al., 2012; Williams et al., 1999). Differences in the composition, rheology, temperature, and pre-existing structures around the triple junction are thought to have contributed to the variability in the evolution of each of the basins.

During the Late Triassic-Early Jurassic (Fig. 4), the rifting apart of Pangaea propagated from south to north and a triple junction formed at the junction between Baltica, Avalonia, and Laurentia (Peace et al., 2019a). Rifting around that triple junction ultimately led to the formation of the East Orphan and Porcupine basins and probably the Galicia Interior Basin (Enachescu et al., 2005; Murillas et al., 1990; Norton, 2002; Shannon et al., 2007; Shannon and Naylor, 1998; Sibuet et al., 2007; Skogseid et al., 2004; Williams et al., 1999). A second rifting phase is marked by the beginning of the clockwise rotation (~43°) of the Flemish Cap, the Porcupine High (~10°), and the Iberian Peninsula (~35° counterclockwise) during the Late Jurassic-Early Cretaceous (Late Cretaceous?), reactivating pre-existing crustal and sedimentary structures (Murillas et al., 1990; Peace et al., 2019b; Sibuet et al., 2007, 2004; van der Pluijm and Marshak, 2004; Vissers and Meijer, 2012). A third rifting phase, associated with the opening of the Labrador Sea, took place during the Late Cretaceous (Abdelmalak et al., 2018, 2012; Keen et al., 2018; Larsen et al., 2009; Peace et al., 2018a), affecting at least the westernmost parts of the West Orphan Basin (Enachescu et al., 2005; Sibuet et al., 2007; Williams et al., 1999).

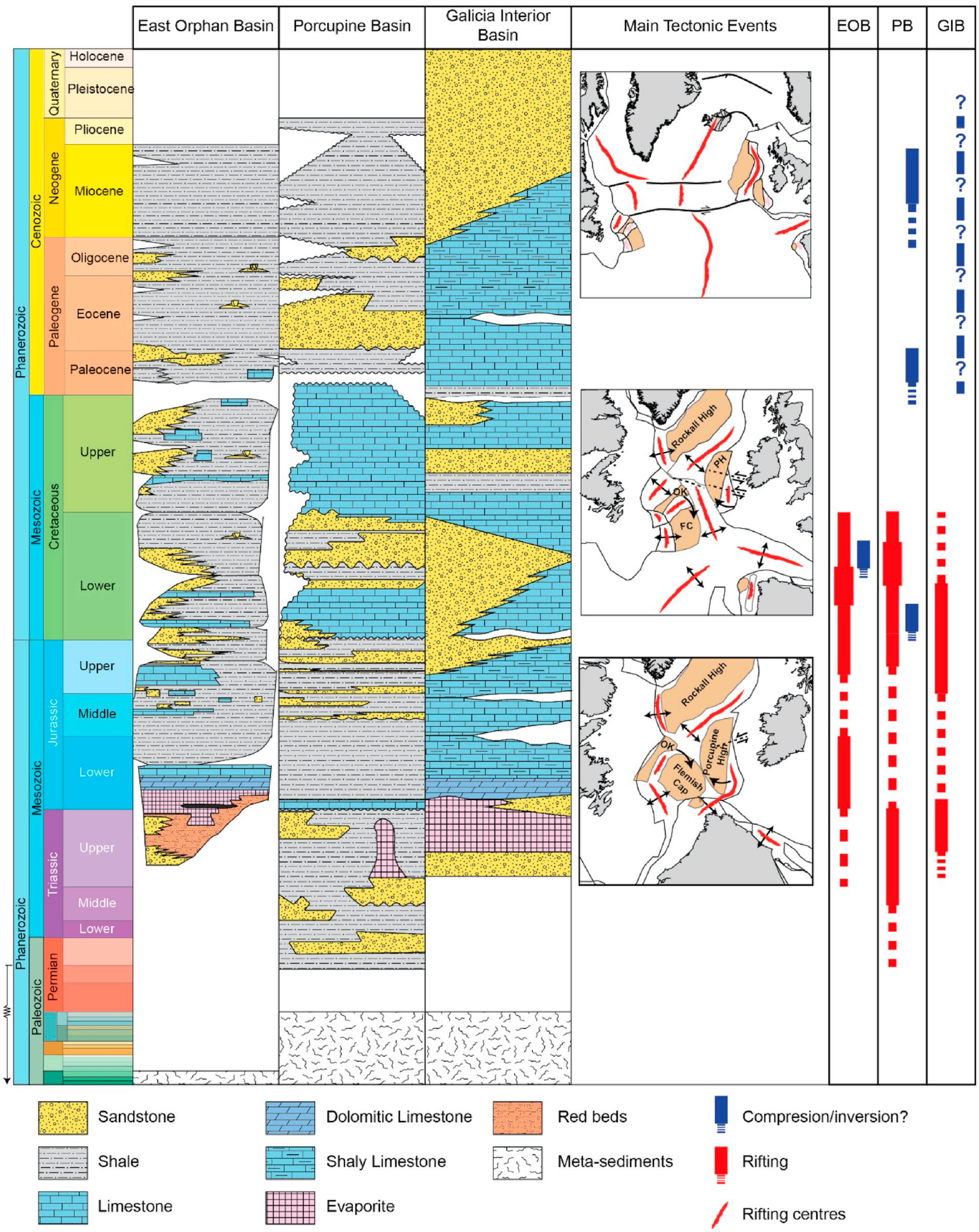

Fig. 4. Simplified lithostratigraphic chart of the East Orphan (BeicipFranlab et al., 2015), Porcupine (Copestake et al., 2018; Shannon et al., 2007), and Galicia Interior basins (Pereira and Alves, 2012). Polygons of schematic main tectonic events adapted from Nirrengarten et al. (2018).

Based on sparse basement drilling and provenance studies, several pre-rift basement terranes have been proposed for the Newfoundland, Irish Atlantic (Tyrrell et al., 2007), and Galicia margins (Fig. 3). The highly stretched East Orphan Basin developed within the Avalon Zone based on its well-preserved upper Precambrian sedimentary and volcanic rocks, which evolved during the Grenvillian-Appalachian time gap, covering Cambrian-Ordovician shales and sandstones (King et al., 1985; Lilly, 1965; Williams, 1979; Williams et al., 1999).

On the Irish Atlantic margin, specific terrane boundaries within the Porcupine Basin are still the subject of active debate (Bluck et al., 1992; Chew and Stillman, 2009; Johnson et al., 2001; Roberts et al., 1999; Tate, 1992; Tyrrell et al., 2007). Nevertheless, terranes of Proterozoic, Avalonian, and Variscan origin have been identified based on geological provenance studies (Tyrrell et al., 2007), outcrops onshore Ireland

(Chew, 2009; Chew and Stillman, 2009; Murphy et al., 1991), and seismic interpretation (Naylor and Shannon, 2005). While the basement terranes of the Iberian Peninsula are generally related to the Variscan Orogeny (Matte, 2001), distinct zones have been defined (Arenas et al., 2004; Farias et al., 1987; Martínez-Catalán, 1990; Murphy et al., 2010) with the Galicia Interior Basin associated with the Galicia-Trás-os-Montes Zone.

The East Orphan Basin is located on the Eastern Canadian continental margin, north of the Grand Banks and southwest of the Orphan Knoll, a fragment of continental crust detached from North America during continental rifting (Keen and Piper, 1990). The Orphan Basin extends over an area of approximately 150,000 km^2 (Department of Mines and Energy, 2000) of which around 33,000 km^2 correspond to the East Orphan Basin. The full Orphan Basin is delimited to the north by the Dover transfer fault and the Charlie-Gibbs Fracture Zone (Keen et al., 1987); to the east by a high basement ridge that runs between Flemish Cap and the Orphan Knoll; to the south by the Cumberland Belt Transfer Zone (Enachescu, 1987), and to the west by the Bonavista Platform (Enachescu et al., 2005; Keen and Beaumont, 1990; Smee et al., 2003). The Orphan Basin is divided into the East Orphan and West Orphan basins based on tectono-structural and petroleum potential analysis (Enachescu, 2006; Enachescu et al., 2005, 2004; Gouiza et al., 2017). The Late Triassic-Early Jurassic marks the beginning of the rifting of the East Orphan Basin whereas the rifting initiation of the West Orphan Basin occurred during the Late Jurassic-Early Cretaceous (Enachescu et al., 2005; Sibuet et al., 2007; Skogseid et al., 2004; Williams et al., 1999).

On the Irish Atlantic margin, the Porcupine Basin is a V-shape trough defined by Naylor et al. (2002) as a Mesozoic-Tertiary basin with a north-south orientation, extending from approximately 50°N northwards to the southern margin of the North Porcupine Basin, north of the Porcupine Arch (Fig. 1b). The basin extends over an area of approximately 44,000 km^2, is delimited to the north and west by the North Porcupine Basin and Porcupine High, respectively, and to the south by the Porcupine Fault and the Goban Spur (Fig. 1). The north and central parts of the Porcupine Basin are characterised by the presence of a deeply buried arch feature (Porcupine Arch) and the Porcupine Median Volcanic Ridge System, respectively (Naylor et al., 2002). The former is defined by Naylor et al. (2002) and described by Johnson et al. (2001) as a high-amplitude reflector which may mark the top of the crystalline crust, and by Gagnevin et al. (2017) as a mafic igneous intrusion situated below the sedimentary cover that could potentially have fed sills at a shallower level. The latter has been interpreted as an igneous complex of mainly Cretaceous age (Tate and Dobson, 1988), a serpentinite-mud volcano or diapir (Reston et al., 2004, 2001), a rotated fault block composed of sedimentary rocks (O'Sullivan et al., 2010a, 2010b), a hyaloclastic mound extruded and deposited close to sea level (Calvès et al., 2012), and a volcanic feature (Watremez et al., 2016).

Along the Iberian margin, the Galicia Interior Basin (GIB) is a U-shaped trough, delimited to the east by the Iberian continental shelf, to the west by the Galicia Bank and the Vigo Seamount, to the north by the Biscay Abyssal Plain, and to the south by the Aveiro Fault and the Porto Seamount (Murillas et al., 1990). Containing a thick sedimentary layer and diapiric structures (Boillot et al., 1979; Groupe Galice, 1979; Mauffret et al., 1978; Montadert et al., 1979, 1974), it is possible that the Galicia Interior Basin is the northward continuation of the onshore Lusitanian Basin (Boillot et al., 1979; Montenat et al., 1988; Wilson et al., 1989). Murillas et al. (1990) suggest that the basin formed during the Triassic with the main extension occurring during the Late Jurassic-Early Cretaceous, similar to the East Orphan and Porcupine basins. Different units have been described for this basin encompassing Jurassic to Cenozoic rocks (Mauffret et al., 1978; Réhault and Mauffret, 1979).

3. Data and methods

The data used in this study include ~22,800 km of 2D pre-stack time-migrated (PSTM) seismic reflection profiles, and well logs and lithological data from 22 wells in the East Orphan, Porcupine, and Galicia Interior basins (Fig. 1). Integration of seismic and well data was performed to define the syn- and post-rift sedimentary packages, and to interpret the large-scale rift- and basement-related faults and geological structures across the Orphan, Porcupine, and Galicia Interior basins.

Well data were provided by the Canada-Newfoundland and Labrador Offshore Petroleum Board (C-NLOPB), the Basin Database of Natural Resources Canada (2017), and the Department of Communications, Climate Action & Environment of Ireland (Fig. 1). No well data from the Galicia Interior Basin are publicly available. However, descriptions and correlations of adjacent wells from the Deep Sea Drilling Project (DSDP), the Ocean Drilling Program (ODP), the Integrated Ocean Drilling Program (IODP), and some industry wells, were made by Sibuet et al. (1979), Boillot et al. (1987), Murillas et al. (1990), and Mena et al. (2018), which are used in this study (Fig. 1).

Seismic lines (EO-1, EO-2, PP-1, PP-2) were provided by TGS-NOPEC Geophysical Company (TGS), the Geological Survey of Canada (GSC), and the Department of Communications, Climate Action & Environment of Ireland. The seismic line that crosses the GIB (GI-1) was digitised and converted into segy format from Pérez-Gussinyé et al. (2003).

Due to the different coordinate reference systems and units used in Canada (North American Datum and Metric system) and Europe (European Datum and Field units), the World Geodetic System 1984 (WGS-84) and the Metric system were used consistently in this study for all of the margins. For the seismic data, positive standard polarity (Sheriff and Geldart, 1995) was used.

3.1. Seismic interpretation

To carry out the seismic interpretation, seismic well ties were built to tie the lithological information from the wells to the seismic data. Having identified the seismic events near the wells, seismic interpretation was performed over the East Orphan, Porcupine, and Galicia Interior basins, by defining five horizons (Cenozoic, Upper Cretaceous, Lower Cretaceous, Jurassic, and Basement) and, based on the seismic stratigraphic character of each layer (Fossen, 2010; Mitchum et al., 1977), three tectonostratigraphic megasequences (post-rift, syn-rift, and pre-rift).

For the East Orphan Basin, the identification of the main seismo-stratigraphic units is based on the integration of the stratigraphic tops from the wells, two computed well ties, and the seismic response of each unit (Fig. 5). Previously published interpretations of Gouiza et al. (2017) were also considered.

For the Porcupine Basin, due to the lack of well data near the seismic lines, the geoseismic sections X, V, and W published by Naylor et al. (2002) were digitised and used as a guide during the seismic interpretation stage. For the Galicia Interior Basin, no well data were publicly available, so the identification of the main seismo-stratigraphic units is based on the work of Murillas et al. (1990) and Pérez-Gussinyé et al. (2003). Since no wells penetrating the deep intervals have been drilled, the reliability of the seismic interpretation at depth is limited where different faulting, rifting, and erosional episodes increase the complexity and therefore the uncertainty.

3.2. Structural restoration

Seismic reflection lines from the East Orphan and Porcupine basins were chosen for structural restoration based on depth-to-basement trends (Divins, 2003; IOC et al., 2003; Oakey and Stark, 1995) and structural elements for the Orphan and Porcupine basins (Edwards et al., 2003; Naylor et al., 2002; Sibuet et al., 2007). The depth to

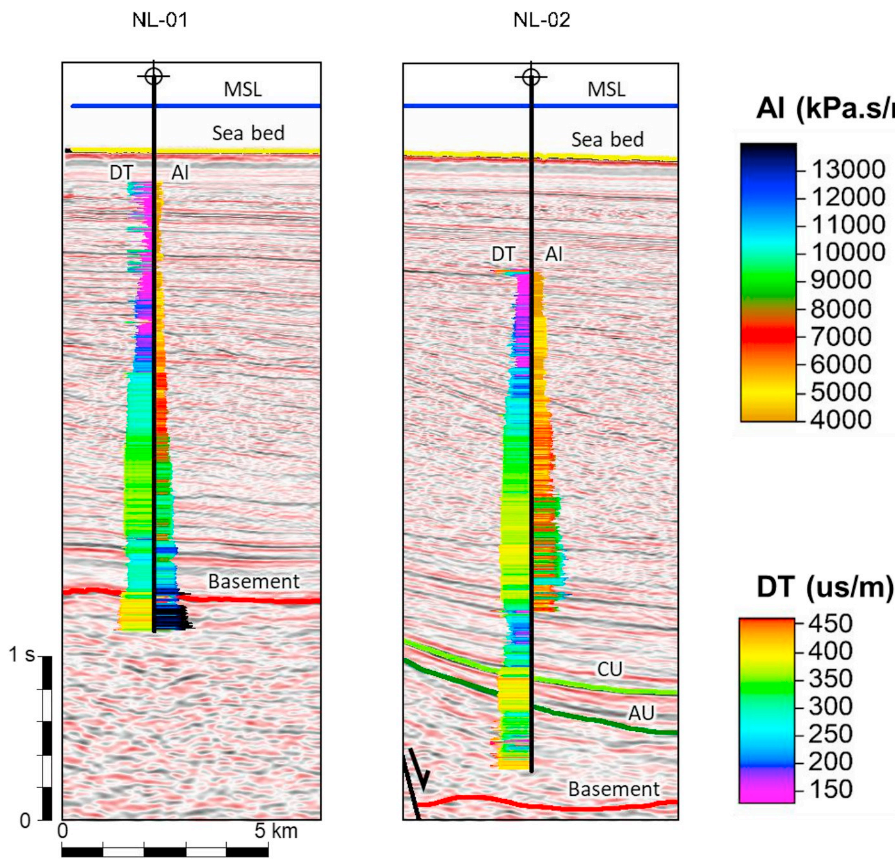

Fig. 5. Examples of seismic–well ties. DT: sonic log; AI: acoustic impedance log. CU: Cenozoic Unconformity. AU: Early Cretaceous Unconformity. See Fig. 1 for location.

basement trends for the Porcupine Basin are based on the General Bathymetric Chart of the Oceans (GEBCO) global 30 arc-second gridded bathymetric dataset (IOC et al., 2003) and total sediment thickness from the National Oceanic and Atmospheric (NOAA) Satellite Information Service (Divins, 2003). For the East Orphan Basin, the depth to basement trends were obtained from the Geological Survey of Canada (Oakey and Stark, 1995). The seismic lines were selected for each basin to capture the maximum dip direction of the general fault trends (Woodward et al., 1989) while also covering the full lateral extent of the basins. The seismic line across the Galicia Interior Basin was not restored due to limited constraints.

Free-air gravity data from the Bureau Gravimétrique International (BGI) (Bonvalot et al., 2012) were also used to visually assess whether the orientations of the chosen seismic lines for restoration were appropriate given the orientations of the main rift features present in the East Orphan and Porcupine basins (Fig. 6). To estimate the depth to the base of the crust, the Mohorovičić discontinuity (Moho) proxy from Welford et al. (2012) and the interpreted Moho from Pérez-Gussinyé et al. (2003) were used.

The interpreted seismic lines for the East Orphan and Porcupine basins were depth-converted using the average interval velocities obtained from the stacking velocities from the Orphan lines (Table 1). The same average velocities were used to depth-convert the Porcupine Basin lines because the average interval velocities are in general agreement with the velocities previously modelled by Readman et al. (2005) and O'Reilly et al. (2006).

The general workflow used to carry out the structural restoration involved: (1) removal of the water layer to decompact the youngest stratigraphic unit, (2) estimation of the isostatic response, (3) for the post-rift units, removal of thermal subsidence effects following decompaction using the estimated beta factor of the crust (β) and rift age, (4) decompaction of the older layers through removal of the youngest stratigraphic unit, (5) for the syn-rift units, restoration of the faults (usually growth faults) to their approximate pre-rifting geometry, (6) if important folds or localised inversion structures are present, unfolding of the units may also be applied, and (7) repetition of this procedure for each interpreted stratigraphic unit. After the fault restoration step and due to the lack of paleo-water depth information for all of the basins, the sections were flattened to a zero datum to better visualise the overall structure and depocentres of the basins. This step does not significantly impact the restoration process since no petroleum system effects are predicted from these restorations. The structural restoration was performed using MOVE™ software by Petroleum Experts Ltd and Midland Valley. For the decompaction process, the porosity-depth function proposed by Sclater and Christie (1980) was used. Appropriate functions are calculated based on the type of lithology present in each layer. The lithological composition used for each unit was estimated by Gouiza et al. (2015) from lithology logs of wells in the Orphan basins (Table 2 and Fig. 7). It is known that the thinning of the crust depends on several factors (rheology, temperature, composition, pre-existing structures, etc.) and is usually modelled using a non-linear viscoelastic material (Lavier and Manatschal, 2006; Naliboff et al., 2017). However, for the pre-rift unit, very low initial porosity and depth coefficient were assumed due to the lack of constraints to define the correct porosity-depth curve for the crust. The difference between not using a decompaction curve for the pre-rift unit (assuming no changes due to removing the upper layers) and the parameters chosen, is on the order of 50 m; therefore, the decompaction of the Jurassic unit does not significantly affect the Basement (crust). Airy isostasy (Airy, 1855) was assumed for both the East Orphan and Porcupine basins to take into account the isostatic response of the lithosphere during decompaction of the sedimentary layers. Despite the three basins in this study being

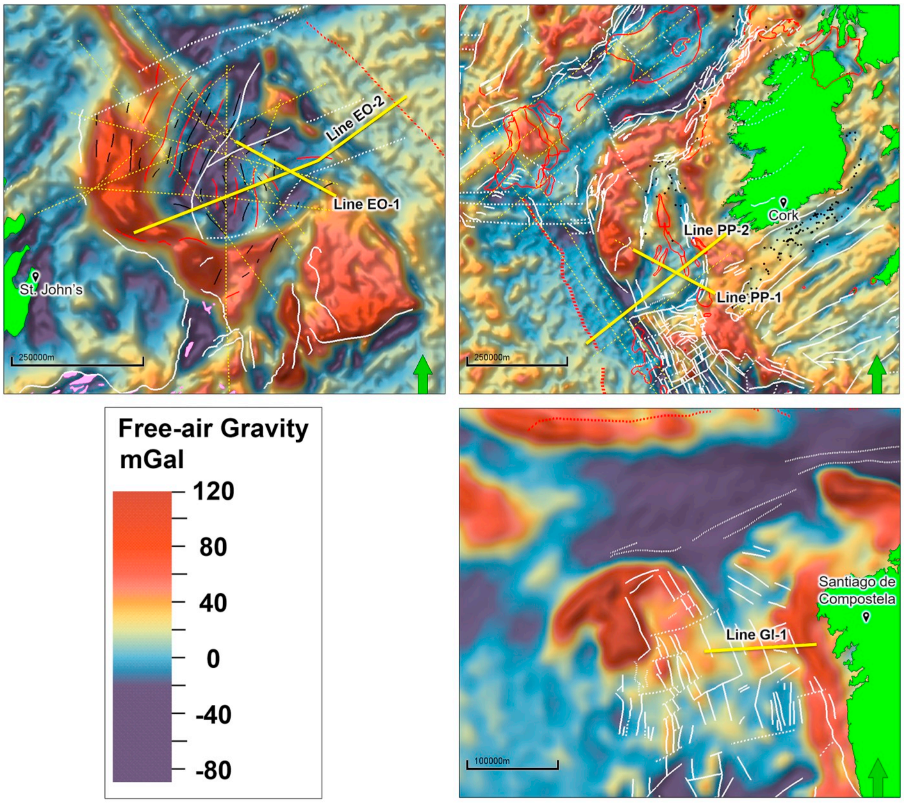

Fig. 6. Free-air gravity anomaly map from Bonvalot et al. (2012). Structural elements adapted from Edwards et al. (2003), Srivastava et al. (1990), Sibuet et al. (2007), Naylor et al. (2002), and Murillas et al. (1990). Continous white lines: normal faults. Dashed white lines: transfer faults. Dotted white lines: inverse faults. Continuous black lines: antiform structures. Solid red lines: synform structures. Solid red polygons: igneous bodies. Dotted red line: magnetic anomaly 34 from Srivastava et al. (1990). Green arrow: north. Green polygons: continent above sea level. Black dots: wells. Dashed yellow lines: available seismic lines. Continuous thick yellow lines: transects interpreted in this study. (For interpretation of the references to colour in this figure legend, the reader is referred to the Web version of this article.)

Table 1
Average interval velocities used for the time-to-depth conversion.

Interval	Average Interval velocity (m/s) – This study	Average Interval velocity (m/s) - Readman et al. (2005)	Average Interval velocity (m/s) - O'Reilly et al. (2006)
Water	1450	1485	–
Cenozoic	2285	2100–2550	~2000
Upper Cretaceous	3238	4000–4100	~3500
Lower Cretaceous	3896	4000–4100	~4000
Jurassic	4718	4500	~5000
Basement	6000–6900	–	~6000
Moho	7200–8000	–	7200–8000

formed by polyphase rifting of a variable duration and intensity, two main rifting episodes are assumed for the restoration. The parameters used to remove the effects of thermal subsidence are shown in Tables 3 and 4. Rather than using a simple constant beta (β) factor for each line, a variable β factor from Welford et al. (2012), derived from constrained 3D regional gravity inversions, was used to capture the highly variable stretching along both the East Orphan and Porcupine lines.

3.3. Kinematic models

The restored sections were spatially tracked through geologic time using the southern North Atlantic plate evolution model from Nirrengarten et al. (2018), constructed using the GPlates[1] software (Boyden et al., 2011). Other published plate reconstruction models are available, such as Seton et al. (2012), Matthews et al. (2016), and Müller et al. (2016); however, the Nirrengarten et al. (2018) model explicitly considers the rotation of the Flemish Cap and the Porcupine High. This is achieved in Nirrengarten et al. (2018) by including independent micro-blocks for the Flemish Cap and Orphan Knoll on the Newfoundland margin and for the Porcupine High, Rockall and Hatton highs on the Irish margin.

The locations of seismic transects EO-1, EO-2, PP-1, PP-2, and GI-1 were imported into GPlates. Plate IDs were then assigned using the static polygons from Nirrengarten et al. (2018). This resulted in the seismic transects EO-1 and EO-2 being assigned to the Orphan Knoll plate (GPlates plate ID 1002), PP-1 and PP-2 to the Porcupine High plate (GPlates plate ID 3001), and GI-1 to the Iberian Peninsula (GPlates plate ID 304). As the plates move through time, the locations of the seismic transects follow the same pole of rotation of the plate they are assigned to. The main drawback of the chosen kinematic model is that it does not take into account the internal deformation of the tectonic plates (Peace et al., 2019b), which is a crucial factor when studying hyperextended basins such as the East Orphan and Porcupine basins. In addition, on rifted margins significant deformation of the continental lithosphere prior to, during, and after breakup is not accounted for in traditional rigid plate models (Peace et al., 2019b). The intensity and direction of stretching in hyperextended basins should be tackled with a non-linear approach that ultimately can reproduce deformation zones akin to the ones defined in the *Crustal Architecture* subsection of this work.

4. Results

4.1. Seismo-stratigraphic units

The selected lines (EO-1, EO-2, PP-1, PP-2, GI-1) were interpreted in two-way travel time (TWT) and five seismo-stratigraphic units were mapped in each basin, namely, Basement, Jurassic, Lower Cretaceous, Upper Cretaceous, and Cenozoic (Figs. 8–11).

4.1.1. Cenozoic

The Cenozoic unit is delimited at the top by an increase in acoustic impedance (the first strong peak) that represents the seabed reflection,

[1] GPlates web site: https://www.gplates.org/.

Table 2
Generic lithological composition of each seismo-stratigraphic unit.

	Sandstone (%)	Shale (%)	Limestone (%)	Porosity at the surface	Depth Coefficient	Compaction Curve
Water	0	0	0	1	NA	NA
Cenozoic	0	80	20	0.59	0.49	Sclater and Christie (1980)
U. Cretaceous	80	10	10	0.50	0.31	Sclater and Christie (1980)
L. Cretaceous	20	80	0	0.60	0.46	Sclater and Christie (1980)
Jurassic	60	30	10	0.52	0.36	Sclater and Christie (1980)
Basement	NA	NA	NA	0.10	0.55	Sclater and Christie (1980)

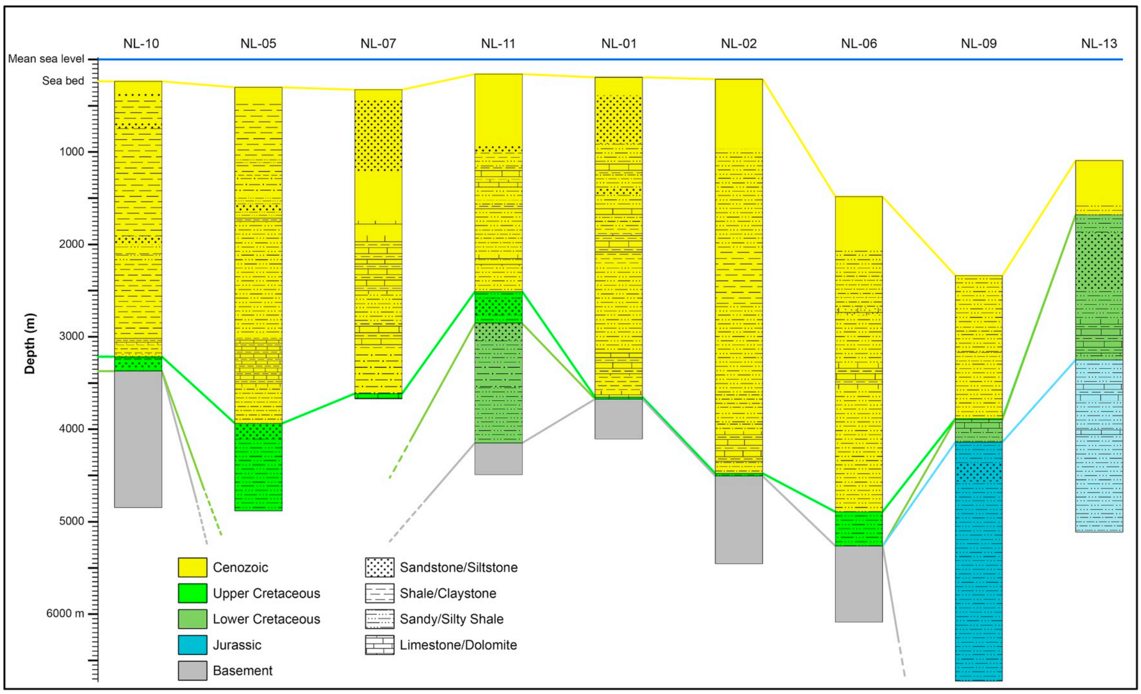

Fig. 7. Generalised lithology based on the descriptions for the cuttings from the wells used in this study. Well locations shown on Fig. 1a.

Table 3
Parameters used to estimate thermal subsidence in the restoration models.

Thickness of lithosphere	125000 m	Morewood et al. (2005)
Initial thickness of continental crust	30000 m	Shannon et al. (1999) Welford et al. (2012)
Mantle density	3300 $^{kg}/_{m^3}$	Gouiza et al. (2015)
Continental density	2800 $^{kg}/_{m^3}$	McKenzie (1978)
Sediment density	2500 $^{kg}/_{m^3}$	
Seawater density	1020 $^{kg}/_{m^3}$	
Thermal expansion coeff. of the mantle and crust	0.000034 $^{1}/_{°C}$	
Temperature of the asthenosphere	1333.0 °C	
Thermal conductivity	1.95 $^{W}/_{(m \cdot K)}$	
Specific heat capacity	0.234 $^{kcal}/_{(kg \cdot K)}$	
Thermal diffusivity	0.0000008 $^{m^2}/_{s}$	
Lithosphere thermal time constant (Tau)	63 Ma	
Extension factor of the lithosphere (β)	Variable	Welford et al. (2012)

and at the base by the Top of the Upper Cretaceous, which corresponds to an unconformity within the East Orphan and Galicia Interior basins. For the East Orphan Basin, the Cenozoic unit is characterised by a relatively continuous parallel to subparallel, sometimes wavy reflection configuration. Some intervals show a more hummocky to chaotic character that could be interpreted either as marine channelised sediments or as mass transport deposits (MTDs). An apparent inversion structure is identified at the southern limit of the basin, indicating that localised uplift occurred during this period. For the Porcupine Basin, this unit exhibits a variable reflection configuration going from subparallel, sometimes wavy, to chaotic. The intervals with the chaotic character may be interpreted either as marine channelised sediments or as MTDs. For the Galicia Interior Basin, the Cenozoic unit is characterised by a variable reflection configuration going from subparallel, sometimes wavy, to chaotic. The chaotic character may correspond to MTDs or marine channelised sediments. Again, an inversion structure is identified at the western end of the seismic line (Fig. 10).

Table 4
Rifting episodes for the East Orphan and Porcupine basins used to estimate thermal subsidence (Gouiza et al., 2017; Shannon et al., 2007; Shannon and Naylor, 1998; Sibuet et al., 2007; Skogseid et al., 2004).

	Rifting Age (Ma)	Duration (Ma)
Lower Cretaceous (K)	125	24.5
Upper Jurassic (J)	163.5	18.5

4.1.2. Upper Cretaceous

The Upper Cretaceous unit is delimited at the top by the base of the

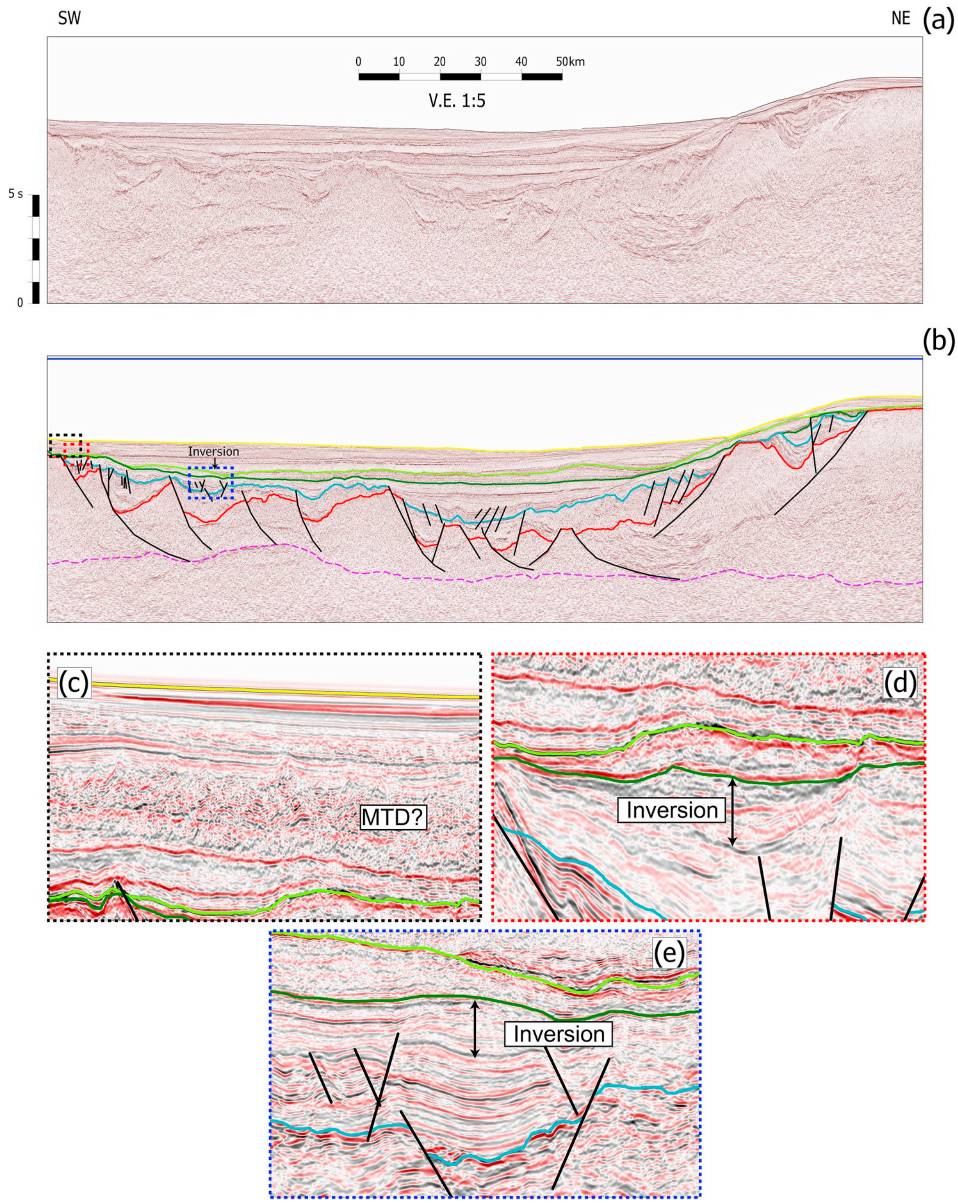

Fig. 8. Seismic line EO-1 with (a) the un-interpreted section and (b) the interpreted horizons. Dark blue line: Mean sea level. Yellow line: sea bed. Light green line: Cenozoic Unconformity. Dark green line: Early Cretaceous Unconformity. Light blue line: Late Jurassic Unconformity. Red lines: basement. Purple line: Moho? (derived from Welford et al., 2012, and seismic interpretation). Dashed boxes in (b) are enlarged below according to the colour of the box outline. See Fig. 1 for location. (For interpretation of the references to colour in this figure legend, the reader is referred to the Web version of this article.)

Cenozoic, a high amplitude positive reflector, and the Early Cretaceous Unconformity at the base. For the East Orphan Basin, the Upper Cretaceous unit exhibits a parallel to subparallel, sometimes discontinuous and wavy reflection configuration. For the Porcupine Basin, the reflection configuration is mostly parallel to subparallel and becomes chaotic towards the flanks of the basin. For the Galicia Interior Basin, this unit exhibits a parallel to subparallel, sometimes discontinuous and wavy reflection configuration that becomes chaotic towards Iberia. The Upper Cretaceous is a post-rift unit that represents the transition from the proper syn-rift deposition during the Lower Cretaceous into a thermal subsidence phase.

4.1.3. Lower Cretaceous

The Lower Cretaceous unit is defined at the top by the Early Cretaceous Unconformity (AU), a positive high amplitude reflector that marks a change in the seismic facies, and at the base by the Late Jurassic Unconformity (TU). For the East Orphan Basin, this syn-rift unit is characterised by laterally continuous, parallel to subparallel, sometimes divergent, reflection character. The section just below the AU, however, exhibits a more wavy to chaotic character. For the Porcupine Basin, the Lower Cretaceous unit is characterised by a variable to wavy subparallel reflection configuration that becomes chaotic on both flanks of the basin. Relatively continuous high amplitude events are evident in the centre of the basin and are interpreted as volcanic intrusions (sills, dykes, or lava flows). For the Galicia Interior Basin, this unit exhibits a highly variable to wavy subparallel, sometimes divergent, reflection configuration that becomes chaotic towards the flanks of the basin. This syn-rift unit shows sedimentary growth towards the normal faults, with apparent inversion structures within all three of the basins of this study (Figs. 8 and 10).

4.1.4. Jurassic

The top of the syn-rift Jurassic unit corresponds to the TU and its base is represented by top basement. Even though the reflection

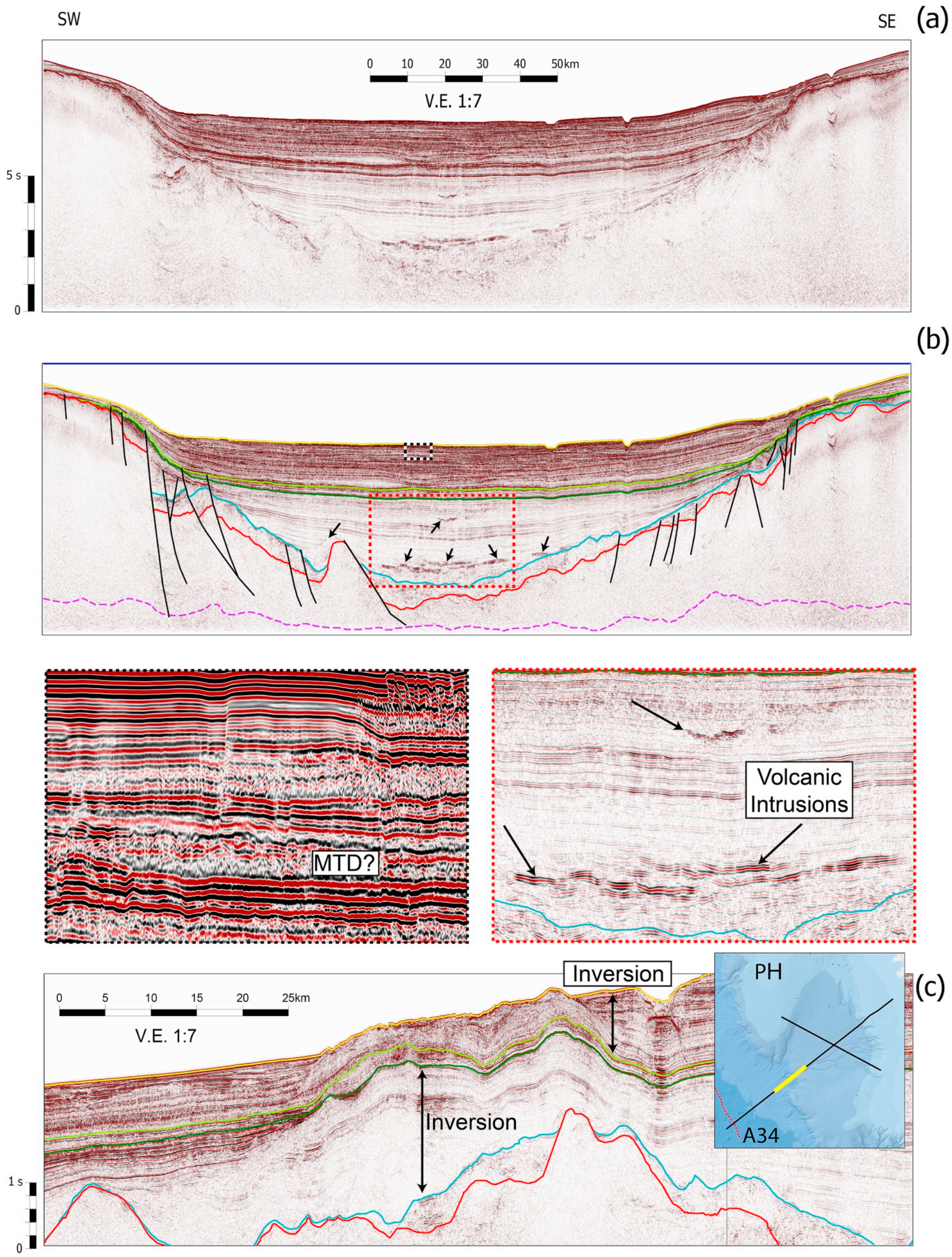

Fig. 9. Seismic line PP-1 with (a) the un-interpreted section and (b) the different interpreted horizons. (c) Inversion structures along seismic line PP-2. Upper Dark blue: Mean sea level. Yellow line: sea bed. Light green line: Cenozoic Unconformity. Dark green line: Early Cretaceous Unconformity. Light blue line: Late Jurassic Unconformity. Red line: basement. Purple dashed line: Moho? (derived from Welford et al., 2012). Black arrows: volcanic intrusions. Dashed boxes in (b) are enlarged below according to the colour of the box outline. See Fig. 1 for location. (For interpretation of the references to colour in this figure legend, the reader is referred to the Web version of this article.)

configuration is highly variable, within the East Orphan Basin two main seismic facies could be defined. The first corresponds to a fairly continuous, parallel to subparallel wavy reflection configuration, with interleaved high amplitude events. The second dominant seismic facies, on the other hand, is composed of chaotic zones that sometimes show internal subparallel reflections. This syn-rift unit is present across the whole basin, except the western-most part of the basin, near the Bonavista platform where this unit seems to be absent. The thickest occurrence of this unit is located in a depocentre in the eastern part of the basin, towards the north of Flemish Cap. The Jurassic unit within the Porcupine Basin is characterised by chaotic reflections with a more subparallel and divergent response on the flanks of the basin. The reflection configuration of the Jurassic unit for the Galicia Interior Basin is variable and sometimes obscured by multiples. Nevertheless, the unit exhibits, overall, a chaotic to divergent reflection configuration. The main depocentre of this unit is located in the central part of the basin, approximately coinciding with the depocentre of the Lower Cretaceous unit.

The uncertainty in the interpretation of the Jurassic unit is moderate to high due to limited well data located on structural highs, the potential structural complexity of this unit, the lower seismic resolution with depth due to signal attenuation, the volcanic intrusions, and the prevalence of multiples. Normal and growth faults, conjugate faults, and rollovers are characteristic of this unit.

4.1.5. Basement

The basal limit of coherent reflections defines the top of the Basement unit. For the East Orphan, Porcupine, and Galicia Interior basins, this seismo-stratigraphic unit is characterised by similar reflection configurations with a chaotic behaviour and virtually no laterally coherent reflections. The imaging of this unit seems to be highly affected by multiples produced by the overlying contrasting layers. Numerous normal and listric faults, tilted fault blocks, and half-grabens are present within this unit. Some of the listric faults sole out at the Moho level. The ages of the basement units have been interpreted to be late Paleozoic (Devonian-Carboniferous) for the Porcupine Basin (Naylor et al., 2002) and early Paleozoic (Ordovician?) for the East Orphan Basin (Koning et al., 1988). For the Galicia Interior Basin, late

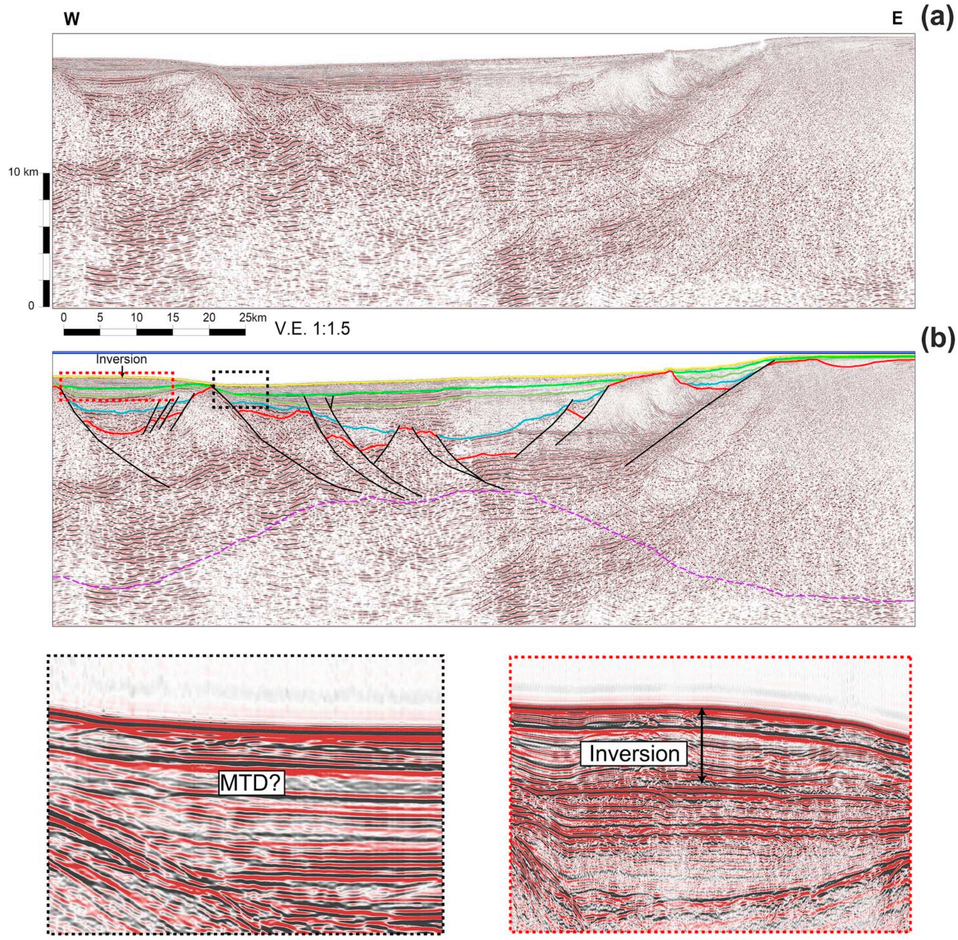

Fig. 10. Seismic line GI-1 with (a) the un-interpreted section and (b) the different interpreted horizons. Dark blue line: Mean sea level. Yellow line: seabed. Light green line: Cenozoic Unconformity. Dark green line: Early Cretaceous Unconformity. Light blue line: Late Jurassic Unconformity. Red line: basement. Purple dashed line: Moho? (derived from Pérez-Gussinyé et al., 2003). Dashed boxes in (b) are enlarged below according to the colour of the box outline. See Fig. 1 for location. (For interpretation of the references to colour in this figure legend, the reader is referred to the Web version of this article.)

Paleozoic is the assigned age for the basement (Groupe Galice, 1979).

4.2. Structural restoration

The structural restoration of the selected lines in the East Orphan and Porcupine basins (Figs. 12 and 13, respectively) shows that evolution, sedimentary cover thickness, and crustal structure of the basins differ significantly (Table 5). The East Orphan Basin shows a more variable and asymmetric crustal structure than the symmetric and elongated Porcupine Basin, with a thicker sedimentary cover found in the Porcupine Basin. The interpreted faulting also reflects these differences, with more variable fault dip direction in the East Orphan Basin compared with the Porcupine Basin. The variation in the fault orientations and dips are due to the different crustal zones experiencing differential extension. The faults closest to the main depocentres and zones with the thinnest crust in each basin, are listric and have shallower dips. Thus, they are likely also harder to detect using seismic methods. Similarly, where the crust is thickest, planar faults are more common. The Lower Cretaceous unit is less affected by faults in all of the basins, indicating either a less accentuated or more distributed rift period, with potentially slow extension rates (hyperextension?). The main Lower Cretaceous depocenters coincide with zones of hyperextended crust (< 10 km).

4.3. Crustal characteristics

The East Orphan Basin, Porcupine Basin, and Galicia Interior Basin have previously been defined as basins with hyperextended crust and partially serpentinised mantle (Calvès et al., 2012; Chen et al., 2018; Lundin and Doré, 2011; O'Reilly et al., 2006; Prada et al., 2017; Reston, 2009; Watremez et al., 2016; Welford et al., 2012, 2010). Consequently, three domains and several subdomains are used to characterise their crustal architecture based on the morphological criteria first proposed by Péron-Pinvidic et al. (2013) and later complemented by Sutra et al. (2013), Chenin et al. (2015), and Chenin et al. (2017).

The different rift domains were interpreted along the same lines that were used for the structural restoration (Figs. 14 and 15). Using published depth-to-basement constraints (Divins, 2003; IOC et al., 2003; Oakey and Stark, 1995), Moho proxy (Welford et al., 2012), interpreted crustal domains (Lundin and Doré, 2011; Welford et al., 2010), and observations generated from this study, maps of the different crustal domains were constructed for the East Orphan and Porcupine basins (Fig. 16).

Along the Newfoundland margin (Figs. 14 and 16a), the proximal domain corresponds to the Bonavista Platform and discrete parts of the Flemish Cap, and is characterised by a crustal thickness from 20 km to more than 30 km and β factors lower than 1.5. Overall, the Flemish Cap is interpreted to be a continental ribbon. This term was first defined by Lister et al. (1986) and later complemented by Péron-Pinvidic and Manatschal (2010). A continental ribbon is a continental block, slightly

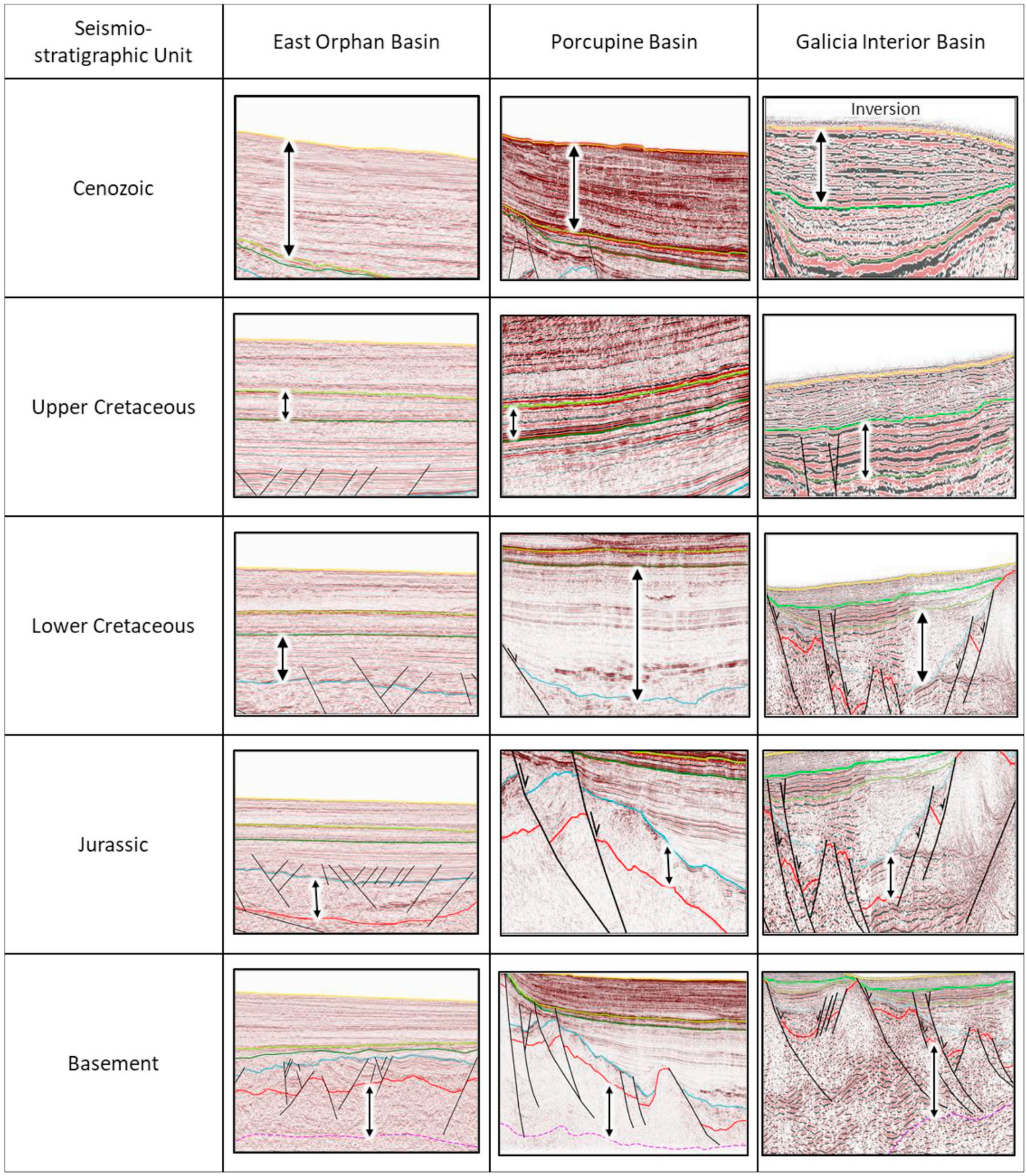

Fig. 11. Examples of seismo-stratigraphic units.

extended, surrounded by weaker zones and still attached to the unrifted continent. Specifically, the Flemish Cap exhibits a crustal thickness of around 20 km and a β factor ranging from 1 to 1.5 containing some localised less stretched areas with thicker crust. This variability in crustal thickness and β factor within the Flemish Cap suggests that it should be modelled as a deformable continental ribbon rather than the classic rigid ribbon part of a larger rigid plate (e.g., Barnett-Moore et al., 2018; Matthews et al., 2016; Nirrengarten et al., 2018; Seton et al., 2012).

The necking subdomain is distributed across both the East and West Orphan sub-basins with a crustal thickness between 10 and 20 km and β factors of 1.5–3.2. A further subdivision of the necking subdomain is used in this study to better delineate the deformation zones between the less stretched distal domain and the highly stretched hyperextended subdomain. These subdomains can be used as deformable zones in deformable kinematic evolution models (e.g., Peace et al., 2019b).

The 1st-degree necking subdomain is characterised by a crustal thickness of 15–20 km and β factors of 1.5–2. This degree of stretching is mild, with no evident faulting present. The 2nd-degree necking subdomain exhibits a crustal thickness of 12–15 km and β factors of 2–2.5. Polyphase faulting becomes important within this subdomain (Reston, 2007) and most of the seismically detectable faults are planar.

The 3rd-degree necking subdomain corresponds to a crustal thickness of 10–12 km and β factors of 2.5–3.2. Here, planar faulting is still significant but listric faulting is increasingly more dominant. Based on this subdivision, the Orphan Knoll falls into the unique category of a continental ribbon with a relatively thin crust (< 20 km) that has been internally deformed.

Two main hyperextended zones are interpreted underneath the depocentres of the West and East Orphan sub-basins (Fig. 16a). A third hyperextended zone is interpreted in the northern part of the Jeanne d'Arc Basin. Based on the interpreted rift domains, at least part of the

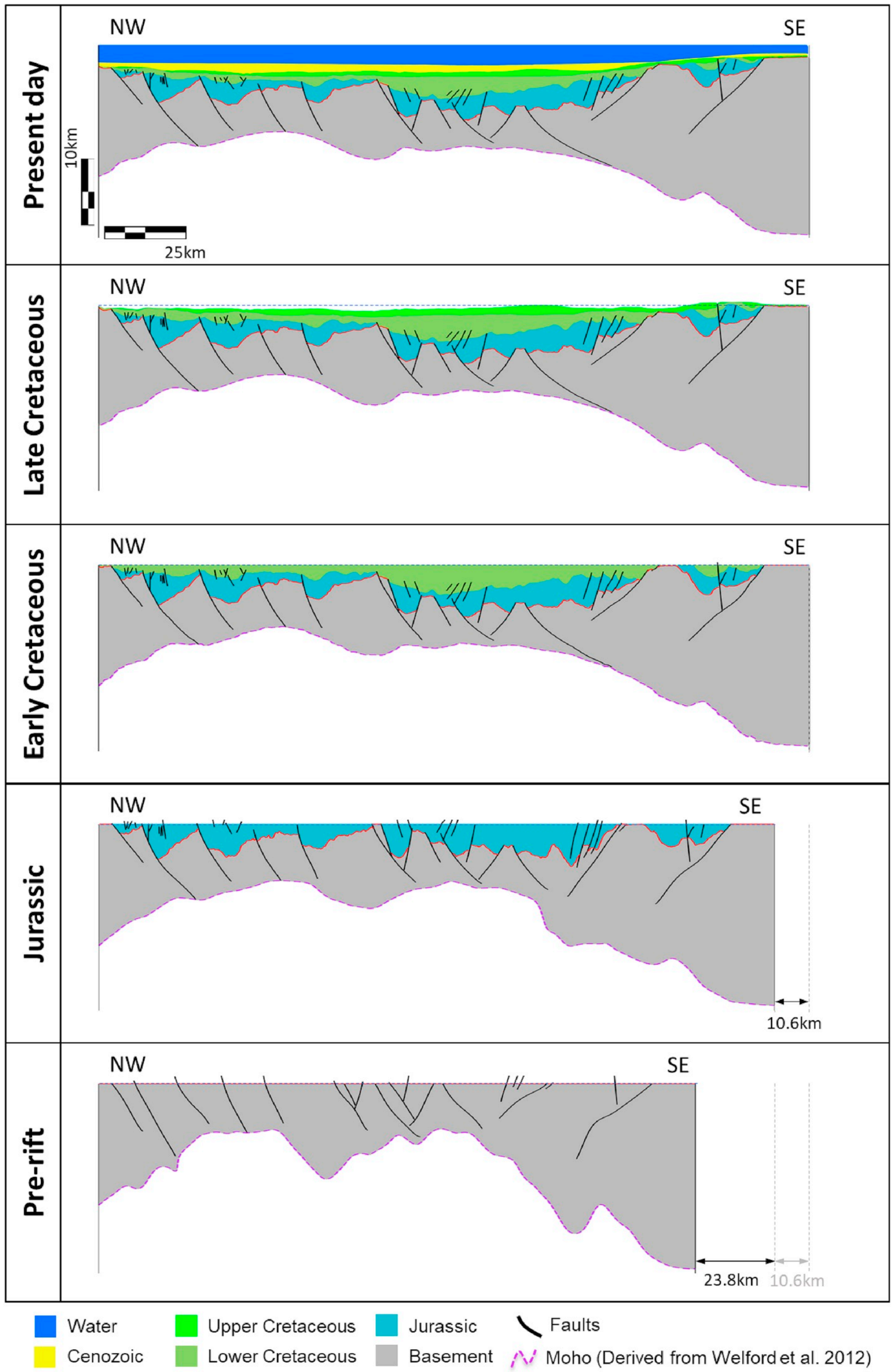

Fig. 12. Structural restoration of line EO-1 across the East Orphan Basin.

White Rose field oil discovery falls inside this hyperextended subdomain (Fig. 16a). With a highly thin crust (down to 4 km thick) and a β factor higher than 3.2 (Pérez-Gussinyé and Reston, 2001), this subdomain exhibits mostly listric faults affecting the Basement unit and planar faults affecting the overlying younger sedimentary units (see EO-1 and EO-2 in Fig. 14). In the West Orphan Basin, the hyperextended subdomain includes a section of the Charlie-Gibbs Fracture Zone (CGFZ) where volcanic intrusions (seamounts?) have been previously interpreted (BeicipFranlab et al., 2016; Keen et al., 2014). The exhumation subdomain on the Newfoundland margin is located just inboard of the oceanic domain and to the east of the Orphan Knoll, where some IODP wells (U1302 and U1303) have been drilled.

Along the Irish margin (Figs. 1, 14 and 156b), the proximal domain is present within some areas of the Porcupine High and the Rockall High, and similar to the configuration observed along the Newfoundland margin, it exhibits a crustal thickness from 20 km to more than 30 km and β factors lower than 1.5. Both the Porcupine High and the Rockall High are interpreted as continental ribbons (Péron-Pinvidic and Manatschal, 2010) with crustal thickness greater than 20 km and β factors of 1.2–1.5, surrounded by more stretched zones (Fig. 16b).

The 1st-degree necking subdomain surrounds the proximal domain in the Porcupine and Rockall basins and has a crustal thickness between 15 and 20 km and β factors of 1.5–2. Only shallow basement-involved planar faults are observed in this subdomain.

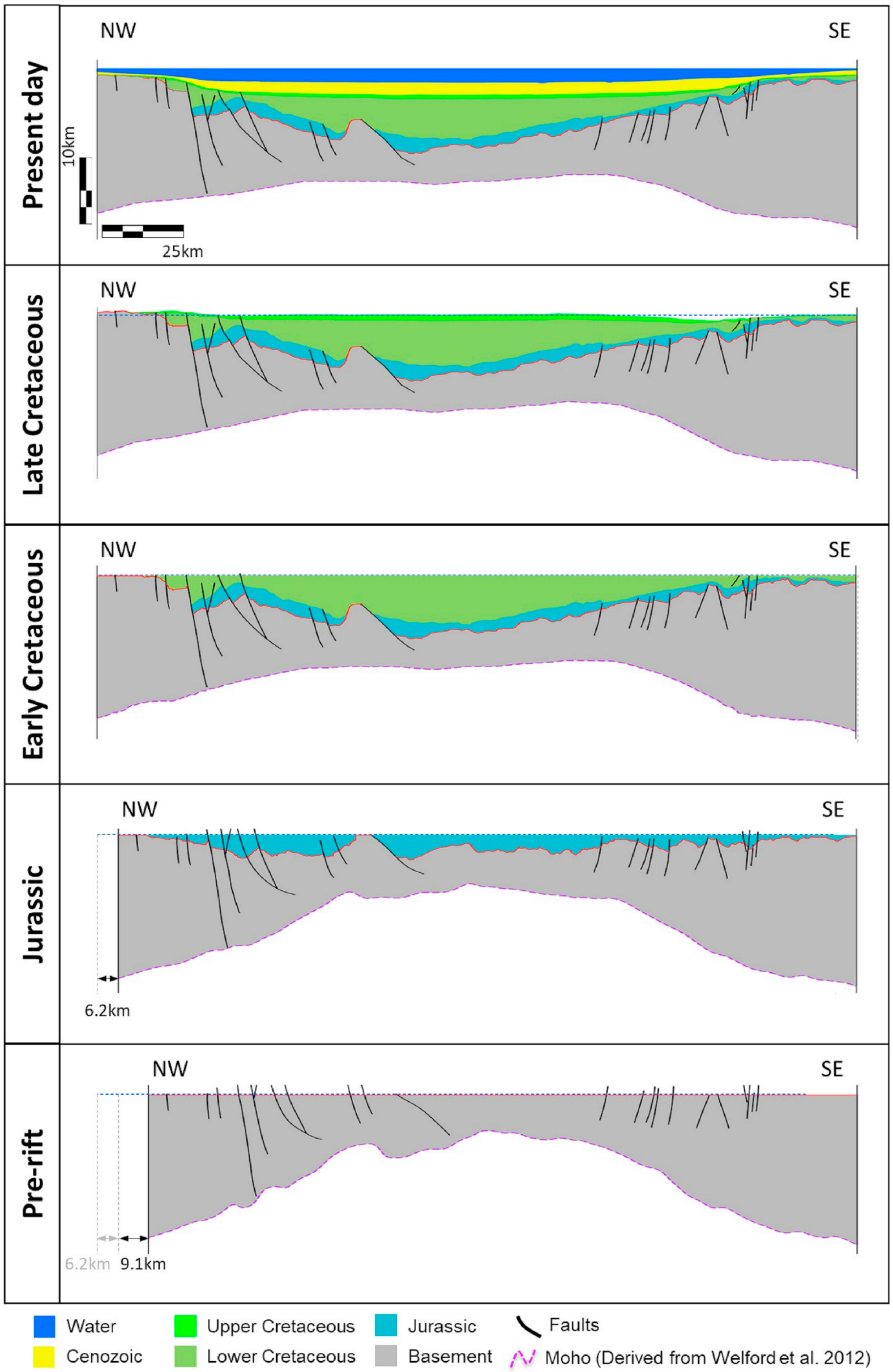

Fig. 13. Structural restoration of line PP-1 across the Porcupine Basin.

The 2nd-degree necking subdomain encompassing the Goban Spur Basin has a crustal thickness between 10 and 15 km and β factors of 2–3.2. Basement-involved listric faults are found in this subdomain with some of them reaching depths close to the Moho. The 3rd-degree necking subdomain surrounds the hyperextended areas within the Porcupine and Rockall basins. It represents a crustal thickness between 10 and 12 km and β factors of 2.5–3.2. Most of the faults are interpreted to be listric with some planar faults.

Two main hyperextended zones corresponding to the main depocentres are also interpreted within the Rockall and Porcupine basins. In the southern part of the Rockall Basin, volcanic intrusions have also been interpreted (Naylor et al., 2002). The exhumation domain is interpreted to correspond to part of the seaward limit of the Rockall Basin, extending towards the south, west of the Porcupine Basin (Fig. 16b). Based on the presence of volcanic intrusions (Naylor et al., 2002) and highly thin crust (down to 6 km thick) with possible serpentinised mantle (O'Reilly et al., 2006), an area of potential exhumed mantle in the central part of the Porcupine Basin is also interpreted.

Along the Galicia margin (Figs. 15 and 16c), the proximal domain is represented by the onshore Iberian Peninsula, the narrow bordering continental shelf, and a small section of the Galicia Bank. It is characterised by a crustal thickness from 20 km to more than 30 km and β factors lower than 1.5. The Galicia Bank exhibits a crustal thickness of up to 20 km and a β factor ranging from 1.2 to 2. Similar to the Orphan

Table 5
Summary of average parameters estimated from the restored sections. Totals are listed in the final row. EOB: East Orphan Basin. PB: Porcupine Basin.

	Thermal Subsidence (m)				Thickness (m)				Extension (km)			
	EOB		PB		EOB		PB		EOB		**PB**	
	EO-1	EO-2	PP-1	PP-2	EO-1	EO-2	PP-1	PP-2	EO-1	EO-2	PP-1	PP-2
Cenozoic	970	986	938	946	1307	2707	1813	1515	–	–	–	–
Late Cretaceous	1182	1138	1180	1122	641	722	558	599	–	–	–	–
Early Cretaceous	–	–	–	–	1657	2077	3300	3109	10.6	13.6	6.5	4.7
Jurassic	–	–	–	–	2450	1868	1552	1421	23.8	29.2	9.3	12.8
Pre-rift	–	–	–	–	11,415	8590	12,080	10,065	–	–	–	–
	2052	**2125**	**2060**	**2126**	-	-	-	-	**34.5**	**43.3**	**15.8**	**17.6**

Knoll, the Galicia Bank is interpreted to be a continental ribbon with a relatively thin crust and internal deformation. The necking subdomain is bordering both the Galicia Bank and the Iberian Peninsula and exhibits a crustal thickness between 10 and 20 km and β factors of 1.5–3.2. The 1st-degree necking subdomain has a crustal thickness between 15 and 20 km and β factors of 1.5–2. Few faults are observed in this subdomain. The 2nd-degree necking subdomain exhibits planar faults and a crustal thickness of 12–15 km and β factors of 2–2.5. The 3rd-degree necking subdomain is barely present on this margin.

Three hyperextended zones are interpreted beneath the Galicia Interior Basin, showing a slightly wider areal extent toward the northern end of the basin (Fig. 16c). Hyperextended zones are also interpreted oceanwards toward the exhumation domain to the west of the Galicia Bank (Fig. 16c).

4.4. Kinematic evolution

The present-day plate configuration (Fig. 17) exhibits the V-shape geometry of the Porcupine Basin and the U-shape configuration of the West and East Orphan basins and the Galicia Interior Basin. A more tabular geometry, however, is exhibited by the Rockall Basin, widening toward its southern limit, near the Charlie-Gibbs Fracture Zone (CGFZ).

Restoring the southern North Atlantic using the Nirrengarten et al. (2018) kinematic model back to the Late Cretaceous (66 Ma), the Labrador Sea was already at an advanced stage of development compared to the Reykjanes Ridge, east of Greenland, that was in an emerging stage. The rotation of the Flemish Cap out of the Orphan Basin and the Porcupine High out of the Porcupine Basin had already occurred. Both the East Orphan and the Porcupine basins are already isolated with no direct connection between them (Fig. 17).

By the Early Cretaceous (100 Ma), the West Orphan Basin and the Rockall Basin appear to be, at least partially, connected (Fig. 17). The Labrador sea rifting is at an incipient stage, and the development of the Reykjanes Ridge has not yet started. To reiterate, by this time the Flemish Cap had already rotated out of the Orphan Basin and the Porcupine High out of the Porcupine Basin, events which are evidently extremely significant to the regional development.

At the end of the Jurassic (145 Ma), the West Orphan Basin was still closed or at an incipient stage (Fig. 17). In other words, most of the extension, the opening of the West and East Orphan basins, and subsequent rotation of the Flemish Cap, have yet to occur. However, the East Orphan Basin was partially formed at this time meaning that its formation is associated with more than one rifting period. Similar to the East Orphan Basin, the Porcupine Basin had started to form at this time. The Nirrengarten et al. (2018) kinematic model shows an offset between the East Orphan and Porcupine basins at this time, while a more continuous and aligned geometry is evident between the Porcupine Basin and the Galicia Interior Basin (GIB).

At the beginning of the Jurassic (200 Ma), the East Orphan Basin was in an early stage of development with a narrower configuration than present. Meanwhile, the Rockall Basin remained wider than the East Orphan Basin. The Flemish Pass, Jeanne d'Arc, East Orphan, and Rockall basins may have formed a continuous system at this time (Peace et al., 2019b). The Porcupine Basin is also at an early stage of basin development, showing a possible connection with the GIB (Fig. 17).

To summarise, the kinematic evolution model of Nirrengarten et al. (2018) shows that the pre-rift connection between the East Orphan Basin and the Porcupine Basin is questionable. Additionally, it shows a potential alignment between the Porcupine and the Galicia Interior basins linking the Flemish Cap with the Porcupine High and the Orphan Knoll with the Rockall High.

5. Discussion

In this section the tectonostratigraphic megasequences, inversion structures, crustal architecture, kinematic evolution, and their interrelation in the evolution of the East Orphan, Porcupine, and Galicia Interior basins are discussed.

5.1. Tectonostratigraphic megasequences

Based on the seismo-stratigraphic characteristics, three tectonostratigraphic megasequences were interpreted. The characteristics of these tectonostratigraphic megasequences are discussed in this section.

5.1.1. Pre-rift

Due to the poorer quality of the seismic data with depth, no pre-rift sediments can be satisfactorily resolved. However, the thickness of the crust is estimated using the interpreted acoustic basement and the Moho proxy from gravity inversion (Welford et al., 2012). The ages for the basement underlying the three basins are similar with the exception of the East Orphan Basin for which an older basement is interpreted (Groupe Galice, 1979; Koning et al., 1988; Naylor et al., 2002). The average thickness of the pre-rift crust is 10 km and 12 km in the East Orphan and Porcupine basins, respectively (Table 5). Both basins contain regions where crust is locally as thin as 3.8 km in the East Orphan Basin and 3.2 km in the Porcupine Basin. Both thin crustal values coincide with highly stretched crust ($\beta = \sim 5$). The East Orphan Basin shows more localised thin crust, coinciding with the location of the two main depocentres, compared with the Porcupine Basin which exhibits one main area of highly thinned crust.

The restored pre-rift crustal section corresponds to the crustal architecture prior to rifting, assuming that all of the extension was due to brittle deformation and has been accounted for. The faulting style in both basins is similar, with normal faults dipping to the west and east on the eastern and western flanks of the basins, respectively. Nevertheless, the greater faulting complexity in the East Orphan Basin indicates either variability during the periods of extension (in magnitude and direction), or a variation in structural (pre-existing structures) and compositional (rheology) inheritance of the crust (more brittle deformation in some areas of the East Orphan Basin compared to the Porcupine Basin).

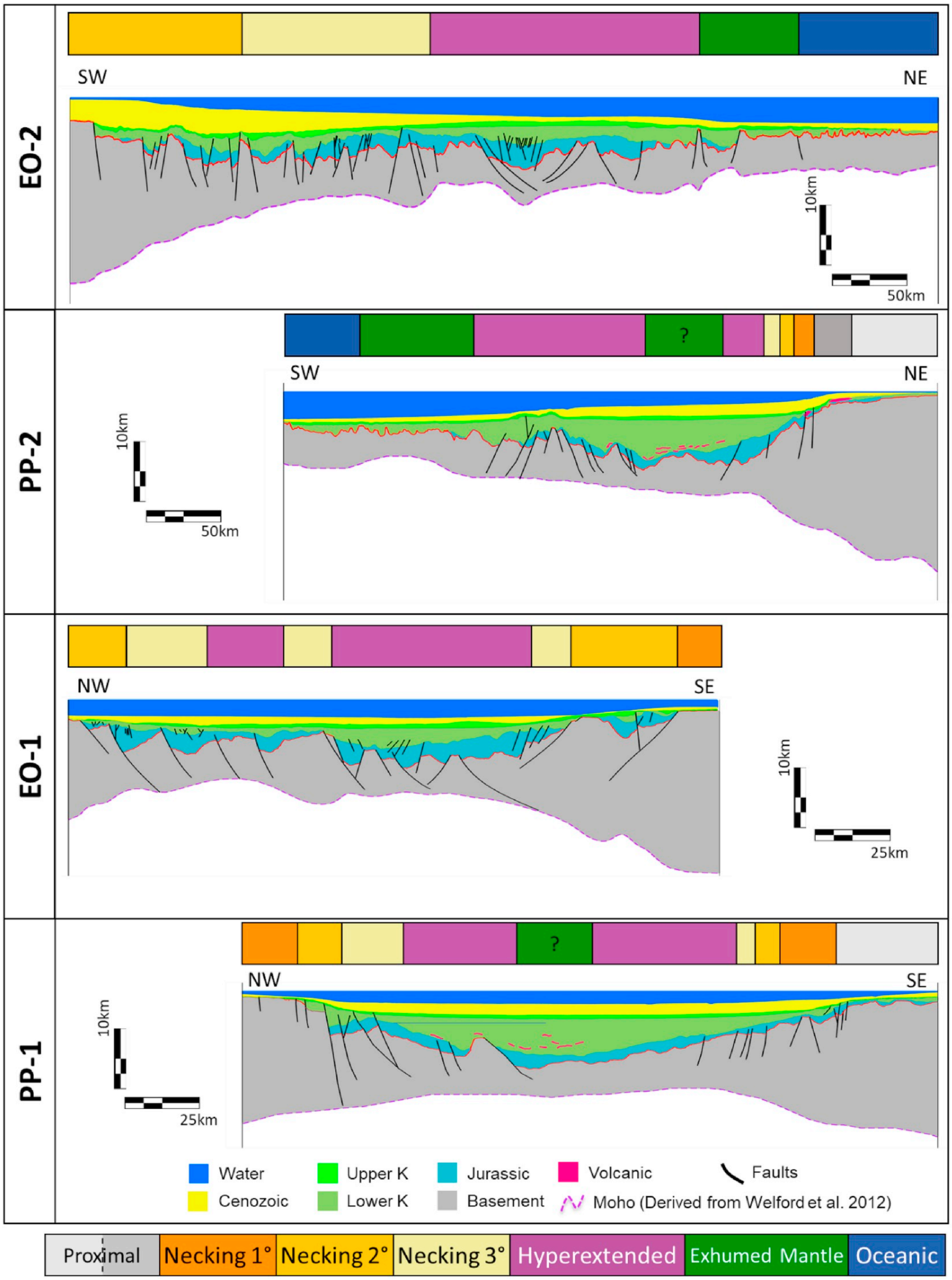

Fig. 14. Geological sections with the interpreted crustal architecture. See Fig. 1 for location.

5.1.2. Syn-rift

The syn-rift megasequence was deposited on the acoustic basement and consists of the Lower Cretaceous and Jurassic units. In the East Orphan Basin, the syn-rift exhibits an asymmetric structural and crustal geometry with several sub-basins (depocentres) defined by rotated fault blocks. The average thickness ranges from 4100 m to 3800 m along lines EO-1 and EO-2, respectively. This asymmetry may reflect variable rheology of the crust, the existence of pre-existing structures within the basin, and/or overprinted intermittent oblique rifting periods. The Porcupine Basin, in contrast, shows a more symmetric geometry with a thicker syn-rift megasequence. The average thickness ranges from 4800 m along line PP-1 to 4200 m along line PP-2 (Table 5). This suggests more continuous deposition of sediments as well as fewer interrupted rifting events.

The restored sections for the syn-rift megasequence reveal at least two main depocentres in the East Orphan Basin. The main depocentre coincides with an area on the eastern flank of the basin with β values higher than 3.5 (hyperextension?) defined by Welford et al. (2012). Whereas on the western flank, several sub-basins (depocentres) are defined by tilted fault blocks.

In the Porcupine Basin, one well-defined depocentre in the central part of the basin is identified along the lines PP-1 and PP-2. This depocentre also coincides with the zone of highest β values (> 3.5) defined by Welford et al. (2012).

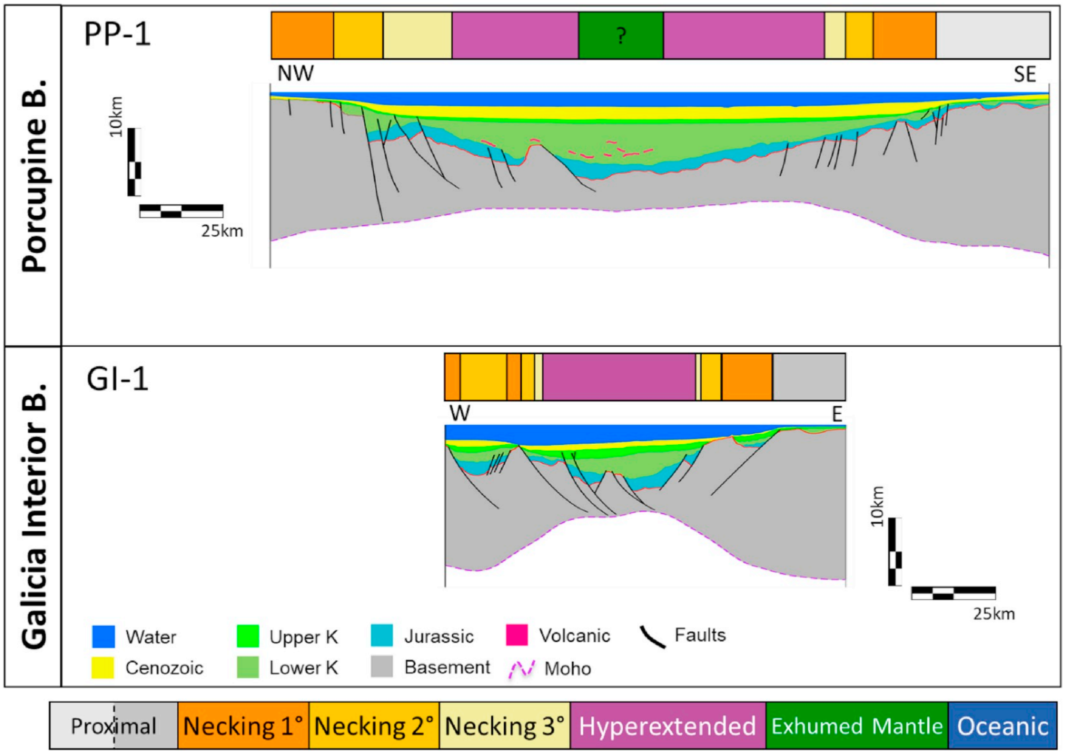

Fig. 15. Comparison of geological sections with interpreted crustal architecture of the Porcupine and Galicia Interior basins. Moho proxy along line PP-1 is derived from Welford et al. (2012) and along line GI-1 is derived from Pérez-Gussinyé et al. (2003). See Fig. 1 for line locations.

Sills, interpreted in this work and in other contributions (Naylor et al., 2002), intrude the Lower Cretaceous unit (Fig. 9). They may be fed by the Porcupine Median Volcanic Ridge and the Porcupine Volcanic Ridge System located just underneath.

The overall structural geometries are also different in each basin. While in the East Orphan Basin, basement-related faults, rotated basement blocks, and syn-depositional tectonic structures are distributed throughout the basin, in the Porcupine Basin, the basement-related

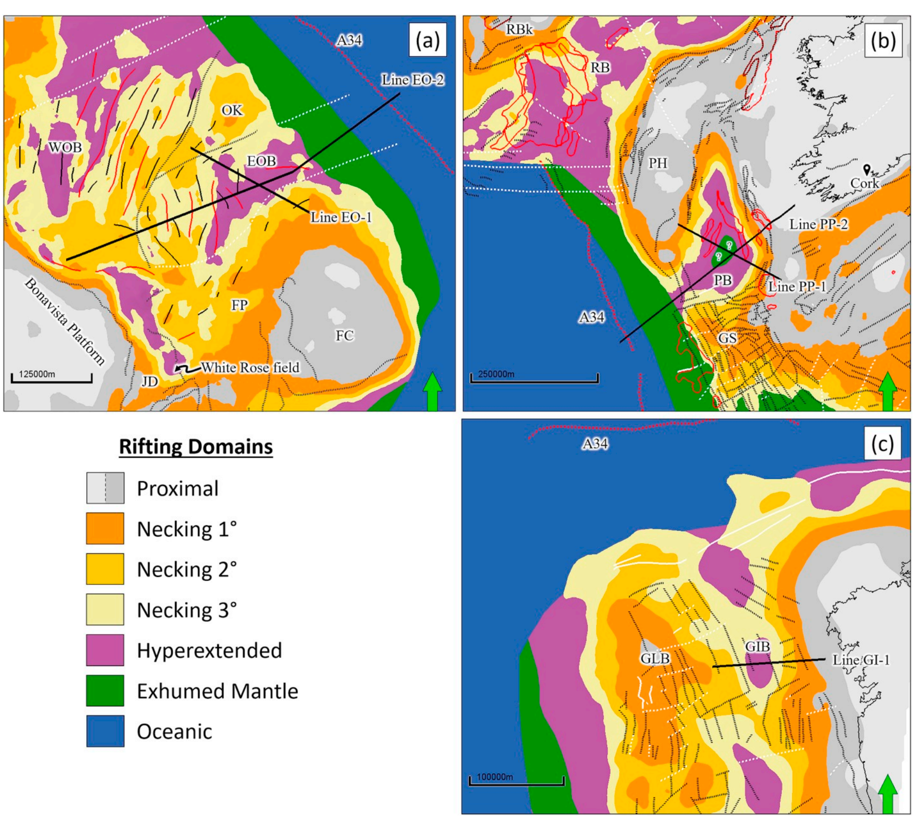

Fig. 16. Maps of the rift domains preserved in the (a) East Orphan and West Orphan basins, (b) Porcupine Basin, and (c) Galicia Interior Basin. Based on the work of Welford et al. (2010), Lundin and Doré (2011), Welford et al. (2012), and observations from this study along the interpreted seismic lines. Structural elements adapted from Edwards et al. (2003), Srivastava et al. (1990), Sibuet et al. (2007), Naylor et al. (2002), and Murillas et al. (1990). Dotted black lines: normal faults/basin edge. Dashed white lines: transfer faults. Continuous thin black lines: antiform structures. Solid red lines: synform structures. Solid red polygons: igneous bodies. Dotted red line: magnetic anomaly 34 from Srivastava et al. (1990). Black dots: wells. Continuous thick black lines: transects interpreted in this study RBk: Rockall Bank. Green arrow: north. See Fig. 1 for legend. (For interpretation of the references to colour in this figure legend, the reader is referred to the Web version of this article.)

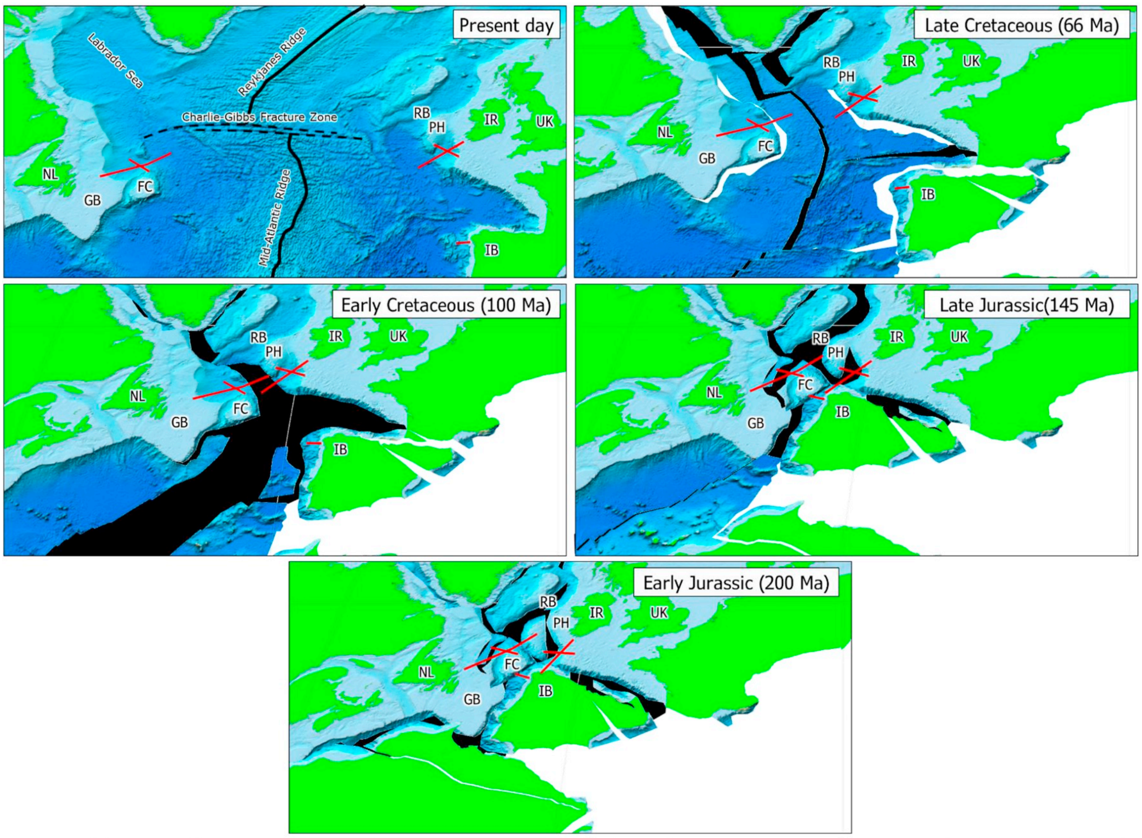

Fig. 17. Location of the interpreted lines (plotted in red) in map view with bathymetry. NL: Newfoundland, FC: Flemish Cap, GB: Grand Banks, IR: Ireland, UK: United Kingdom, RB: Rockall Basin, IB: Iberian Peninsula. Black solid line/polygon: rift location. Kinematic evolution model from Nirrengarten et al. (2018).

faults are more common on the basin flanks, rotated basement blocks are mostly associated with the structural basement high at the southern limit of the basin, and the syn-depositional tectonic structures are less pronounced. For the Jurassic unit, the crustal extension estimated from the restoration varies from 23.8 km (EO-1) in the East Orphan Basin to 9.3 km (PP-1) in the Porcupine Basin (Table 5). This indicates that most of the important extension occurred during the Jurassic, significantly affecting the East Orphan Basin. Furthermore, the estimated horizontal extension is approximately 10.6 km (line EO-1) in the East Orphan Basin and 6.5 km (line PP-1) in the Porcupine Basin. This suggests that the extension associated with the Lower Cretaceous was higher in the East Orphan Basin than in the Porcupine Basin. Based on the thickness variability of each sedimentary unit, the structural style, and the amount of extension, the possible connectivity between the East Orphan and the Porcupine basins during rifting is not evident.

5.1.3. Post-rift

The post-rift megasequence is represented by the Cenozoic and Upper Cretaceous units. The base of this megasequence (~100.5 Ma) marks the beginning of the break up between Europe and North America (Seton et al., 2012). During the deposition of this megasequence, the basins evolved from active rifts until the end of the Early Cretaceous, to a passive setting when rifting ceased in the Late Cretaceous and Cenozoic. Thick sedimentary packages were deposited during this period. In the East Orphan Basin, the average thickness of this megasequence is between 1300 m along line EO-1 and 2700 m along line EO-2. Whereas in the Porcupine Basin, the average thickness is between 1500 m and 1800 m along lines PP-2 and PP-1 (Table 5). The structural architecture of the basins is similar. The East Orphan and the Porcupine basins exhibit a symmetric geometry, with thicker post-rift in the East Orphan Basin. This difference in thickness may suggest two scenarios: (1) more sedimentary sources available to fill the basin, or (2) similar amounts of sediment availability but a narrower accommodation space to be filled in the East Orphan Basin. The second scenario seems to be more reasonable since the Porcupine Basin has a wider area (~70,000 km^2) than the East Orphan Basin (~33,000 km^2).

5.2. Inversion structures

Inversion structures are identified along the East Orphan, Porcupine, and Galicia Interior basins. Despite their relatively small scale (20–30 km wide), they should be considered to better understand the formation and evolution of these three basins. In the East Orphan Basin, the inversion structures are localised in the central and northwestern parts of the basin. These inversion structures (up to 30 km wide) are observed in Early Cretaceous rocks. Early Cretaceous inversion has been identified in other places within the East Orphan Basin (Thompson, 2003), indicating a high variability of extension and deformation that is characteristic of oblique extensional regimes. For the Porcupine Basin, an apparent inversion structure (~20 km wide) embedded in Cenozoic (Late Cretaceous-Paleogene?) rocks is identified at the southern limit of the basin. Previous studies have interpreted this feature (Masson and Parson, 1983; Naylor et al., 2002) assigning a late Eocene age (Masson and Parson, 1983). In the Galicia Interior Basin, an inversion structure (~17 km wide) within Cenozoic rocks (Paleocene?) is identified at the western end of the basin. Inversion structures of Cenozoic age have been previously interpreted at the north-eastern end of the Galicia Interior Basin. However, they are associated with formation of underlying seamounts (Murillas et al., 1990).

The apparent timing difference in the formation of the inversion structures along the East Orphan, Porcupine, and Galicia Interior basins could be explained by two scenarios: (1) for the East Orphan and Porcupine basins, different formation mechanisms (direction and timing of extension) led to the development of these basins, and (2) the basins were formed in a regional oblique extensional regime with varied extension directions along each margin.

5.3. Crustal architecture

The interpreted crustal characteristics for the East Orphan, Porcupine and Galicia Interior basins seem to have some common characteristics. The rift domains seem to be controlled by the presence of pre-existing structures (Fig. 3). The limits of these potential pre-existing structures (e.g., a change from Variscan to Caledonian basement between the Porcupine and Rockall basins) are considered zones of localised rifting within the broader diffuse rifting zone (Bulois et al., 2018), producing zones of hyperextension as seen in the East Orphan, Porcupine, and Galicia Interior basins (Fig. 16).

The axial depocenters for the syn-rift units partially coincide with the overall depocenters of the basins. This suggests that while regional diffuse rifting was taking place, localised rifting was occurring due to local variations in crustal composition (rheology). This polyphase rifting scenario explains the apparently continuous and more intense stretching (hyperextension) in the areas affected by multiple diffuse rifting episodes.

Due to similar basin geometries and basement ages (Devonian-Carboniferous), we infer that the Porcupine and Galicia Interior basins were formed through a similar extension mechanism with a diffuse rift propagating from the Galicia Interior Basin into the Porcupine Basin. Their crustal structures also show similar axial and partially symmetrical hyperextended zones with the only difference being the igneous centres present in the Porcupine Basin (e.g., PMVR). The igneous centres in the Porcupine Basin are thought to have formed during the Early Cretaceous with a later intrusive phase during the Cenozoic (Naylor et al., 2002).

5.4. Conjugate or contemporaneous basins?

The evolution of the Atlantic margins of Newfoundland and Ireland has been the subject of numerous investigations (Burk and Drake, 1974; Doré et al., 1999; Kristoffersen, 1978; Lundin, 2002; Skogseid, 2010; Srivastava et al., 1990, 1988; Srivastava and Verhoef, 1992; Welford et al., 2012, 2010; Ziegler, 1988, 1982). Some paleoreconstructions of the North Atlantic Ocean show the East Orphan and Porcupine basins forming a continuous basin despite fundamental differences in their evolution, structural style, sedimentary thickness, and amount of volcanic intrusions (e.g., Knott et al., 1993; Skogseid, 2010).

Having restored the interpreted geological cross-sections of the East Orphan and Porcupine basins (Figs. 12 and 13), the overall results for both basins are summarised in Table 5. Thermal subsidence amounts are similar for both basins, with the exception of the β factors that vary within each basin.

Sedimentary thicknesses are different, with thicker sedimentary cover in the Porcupine Basin during the Cenozoic, and similar thicknesses in both basins during the Upper Cretaceous. The most significant thickness difference is observed for the Lower Cretaceous unit, which is ~1400 m thicker in the Porcupine Basin than in the East Orphan Basin. For the Jurassic unit, the opposite is observed, as the East Orphan Basin exhibits a thicker sedimentary layer than the Porcupine Basin.

Due to the differences in thickness, the Porcupine Basin, compared with the East Orphan Basin, can be defined as a nourished basin. In terms of crustal thickness, the average thickness is higher in the Porcupine Basin, but both basins contain areas with highly thinned crust of less than 6 km (O'Reilly et al., 2006; Welford et al., 2012).

The amounts of brittle extension are also different in both basins, with more extension (~34.5 km) observed in the East Orphan Basin (along the line EO-1) than in the Porcupine Basin (15.8 km along the line PP-1). The amounts of extension predicted by the Nirrengarten et al. (2018) kinematic evolution model (Table 6) are significantly higher. These amounts were estimated in GPlates by defining points at the end of each line, anchoring these points to their respective plate ID, and measuring the distance between the points as the model changes through time. Observed differences between the Orphan and Porcupine basins may be a consequence of several factors: (1) variable composition/rheology of the crust beneath both basins, (2) variable thinning factor of the lithosphere (β > 2) with seismically undetectable (polyphase faulting) listric subhorizontal faulting and depth-dependent stretching occurring in varying degrees across either basin, and (3) highly oblique extension that could have contributed to the formation of both basins (e.g., rotation of the Flemish Cap and Porcupine High out of the Orphan and Porcupine basins, respectively). The latter scenario would generate 3D stress and strain fields that would vary depending on the direction of measurement, resulting in significant obliquity, as already predicted for the margins (Brune et al., 2018). Thus, the extension estimated in this study would need to be used as a vector component to estimate the correct amount of extension in a required direction.

Table 6
Amount of extension extracted from the Nirrengarten et al. (2018) kinematic evolution model.

	Extension (km)			
	EO-1		PP-1	
	Nirrengarten et al. (2018)	This work	Nirrengarten et al. (2018)	This work
Cenozoic	–	–	–	–
Upper Cretaceous	–	–	–	–
Lower Cretaceous	14.3	10.6	7	6.5
Jurassic	73	23.8	75	9.3
Pre-rift crust	–	–	–	–
	87.1	**34.5**	**82**	**15.8**

Based on the characteristics summarised above, the potential linkage between the East Orphan and the Porcupine basins seems implausible. Therefore, the East Orphan and Porcupine basins should be considered as contemporaneous basins located on conjugate margins rather than conjugate basins.

5.5. Galicia Interior basin: a continuation of the Porcupine Basin?

The kinematic evolution models of Nirrengarten et al. (2018) and Matthews et al. (2016) place the Porcupine Basin relatively aligned and continuous with the Galicia Interior Basin (Fig. 18). Due to this potential connectivity, the seismic line GI-1, located along the Galicia Interior Basin (Fig. 1), was compared with line PP-1 from the Porcupine Basin. The age of each sedimentary unit within the Galicia Interior Basin is based on the information published by Murillas et al. (1990) and Pérez-Gussinyé et al. (2003), and the interpretation followed the same methodology applied to the Orphan and Porcupine seismic lines (Fig. 15).

Line GI-1 across the Galicia Interior Basin has previously been interpreted by Pérez-Gussinyé et al. (2003). Despite differences in basin width, the Porcupine and Galicia Interior basins show similar basinal and crustal structures, with relatively symmetric geometries and well-defined depocentres located in the central parts of the basins. The average crustal thickness along line GI-1 is 13.3 km with a highly thinned crust (~4 km) in the central part of the basin and thicker crust (15–20 km) at the edges of the basin (Pérez-Gussinyé et al., 2003).

Along line GI-1, the sedimentary thickness is noticeably different, with thinner sedimentary layers for the Cenozoic and Lower Cretaceous units but thicker layers for the Lower Cretaceous and Jurassic units. The variation in sedimentary thickness could be associated with the different basin widths, with more accommodation space available in the Porcupine Basin, and/or different sediment sources.

Based on the kinematic evolution models of Nirrengarten et al.

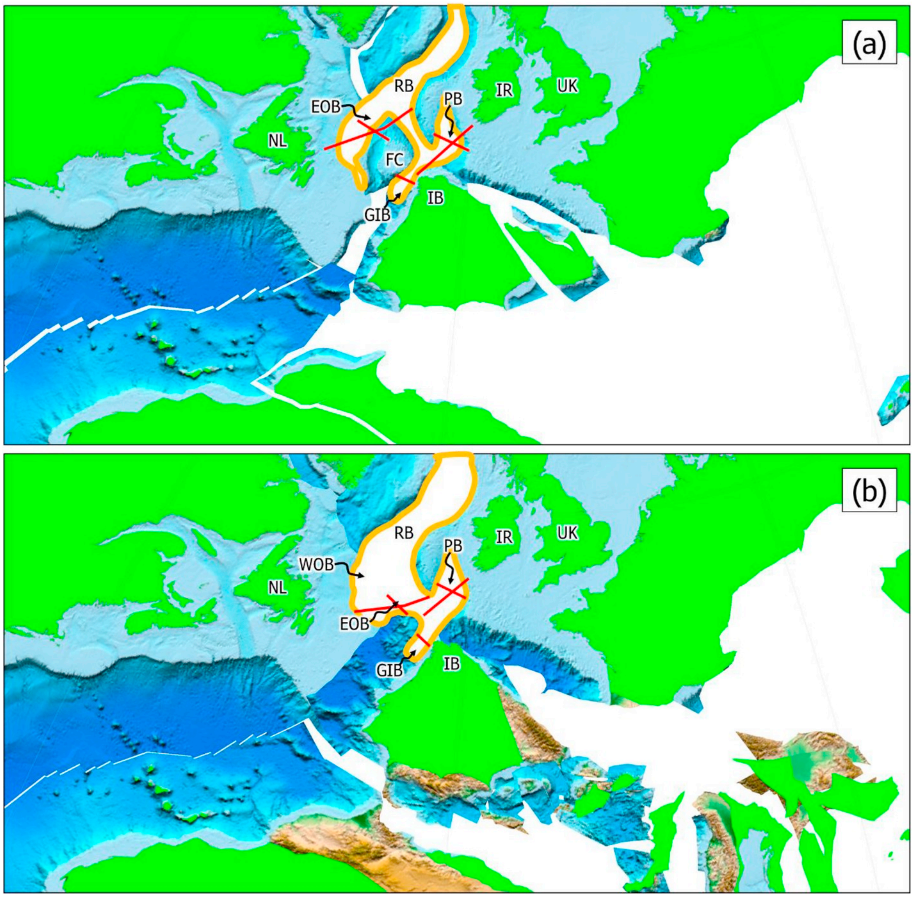

Fig. 18. Kinematic evolution models showing the potential link between the Porcupine and Galicia Interior basins at the end of the Jurassic (145 Ma). (a) Nirrengarten et al. (2018). (b) Matthews et al. (2016). WOB: West Orphan Basin. EOB: East Orphan Basin. RB: Rockall Basin. PB: Porcupine Basin. GIB: Galicia Interior Basin. FC: Flemish Cap. IB: Iberia Peninsula. Orange lines: basin boundaries. Red continuous lines: seismic lines analysed in this study. Green polygons: continent above sea level. (For interpretation of the references to colour in this figure legend, the reader is referred to the Web version of this article.)

(2018), Peace et al. (2019b), and Matthews et al. (2016), the Galicia Interior Basin and the Porcupine Basin formed a continuous basin during the Jurassic period (Fig. 18). However, the only apparent similarity between the basins is their general structure. A rift propagation (Bulois et al., 2018; Chen et al., 2018) from the Galicia Interior Basin into the Porcupine Basin during the Jurassic would explain the structural similarities. Later, during the Early Cretaceous, the opening of the Bay of Biscay (Gong et al., 2008) interrupted the propagation of the rift, separating the Galicia Interior and Porcupine basins.

If the Galicia Interior Basin and the Porcupine Basin formed a continuous elongated basin during the Jurassic (Fig. 18), the direction and amount of extension, timing of rifting, micro-plates involved and their internal deformation, must all be taken into account in kinematic evolution models that incorporate deformation (e.g., Peace et al., 2019b). Such deformable models are required to reproduce and understand the relationship between the basins as well as the Bay of Biscay triple junction around which they all evolved simultaneously (Peace et al., 2019b; Sibuet and Collette, 1991).

5.6. Petroleum system implications

The potential connectivity of these basins has important implications for hydrocarbon exploration. Although the aim of this work was not to carry out a full petroleum system evolution analysis, implications in terms of source rock presence and thermal maturity can be extracted from the results of this study. Traditional basin evolution models are based on uniform beta factors and present-day topography of the basement. For the case of hyperextended basins, the authors suggest (1) incorporating variable beta factors (e.g., Welford et al., 2012) and (2) using estimates of paleotopography. These suggestions as applied to basin modelling will help to produce better estimates for heat flow, therefore reducing the uncertainty of the thermal history of sediments (Watremez et al., 2016), to better predict shale- and sand-prone zones, and to define potential hydrocarbon traps.

6. Conclusions

Interpretation of PSTM seismic reflection profiles along the East Orphan, Porcupine, and Galicia Interior basins, and structural restoration of select lines, were integrated with crustal-scale geophysical datasets and kinematic evolution models to carry out an integrated comparison of the East Orphan, Porcupine, and Galicia Interior basins. The key findings of this work include the following:

(1) The East Orphan Basin exhibits a complex distribution of sediments with several depocentres or sub-basins. By comparison, the Porcupine and Galicia Interior basins form more symmetric basins with only one, centrally located depocentre.
(2) Localised inversion structures were identified along the East Orphan (Early Cretaceous?), Porcupine (Late Cretaceous-Paleocene?), and Galicia Interior (Paleocene?) basins, potentially indicating localised zones of compression in a regional oblique extensional regime.
(3) Based on the similar estimated ages of the interpreted seismostratigraphic units and the crustal architecture of each of the basins, the rifting events that affected the East Orphan, Porcupine, and Galicia Interior basins are interpreted to be synchronous and similar.
(4) The variations in the crustal characteristics, the sedimentary cover thicknesses, and plate kinematic models suggest that highly oblique intermittent diffuse rifting events affected the East Orphan Basin whereas the Porcupine Basin could potentially have been affected by fewer interrupted, more localised rifting events.
(5) The different amount of extension, the distribution of rifting

domains, and the broad crustal architecture of the East Orphan, Porcupine, and Galicia Interior basins, along with the evolution models of Nirrengarten et al. (2018) and Matthews et al. (2016) indicate that the connection between the East Orphan and the Porcupine basins is unlikely, but rather ancient connections between the Porcupine and Galicia Interior basins, and the East Orphan and Rockall basins during the Early to Late Jurassic, are proposed.

Building a kinematic evolution model that takes into account internal deformation of the crustal domains defined in this study as well as pre-existing structures associated with ancient orogenic events would provide a better estimate and understanding of the amount of extension and current structures present along and surrounding not only the Newfoundland, Irish, and Iberian conjugate margins but also any kinematic evolution studies around triple junctions.

Acknowledgements

Data for this study were provided by TGS-NOPEC Geophysical Company (TGS) and the Department of Communications, Climate Action & Environment of Ireland. The research was funded by Innovate NL. Petroleum Experts Ltd. and Midland Valley provided the academic licence for the MOVE™ software, Schlumberger provided the licence for the Petrel software, and Esri provided the ArcGIS academic licence. Alexander L. Peace's Postdoctoral Fellowship at Memorial University of Newfoundland was funded by the Hibernia Project Geophysics Support Fund and Innovate NL. The authors acknowledge the constructive and helpful reviews of Cédric Bulois, Mohamed Gouiza, and an anonymous reviewer.

References

Abdelmalak, M.M., Geoffroy, L., Angelier, J., Bonin, B., Callot, J.P., Gélard, J.P., Aubourg, C., 2012. Stress fields acting during lithosphere breakup above a melting mantle: a case example in West Greenland. Tectonophysics 581, 132–143. https://doi.org/10.1016/j.tecto.2011.11.020.

Abdelmalak, M.M., Planke, S., Polteau, S., Hartz, E.H., Faleide, J.I., Tegner, C., Jerram, D.A., Millett, J.M., Myklebust, R., 2018. Breakup volcanism and plate tectonics in the NW Atlantic. Tectonophysics. https://doi.org/10.1016/j.tecto.2018.08.002.

Airy, G.B., 1855. On the computation of the effect of the attraction of mountain-masses, as disturbing the apparent astronomical latitude of stations in geodetic surveys. Phil. Trans. Roy. Soc. Lond. 145, 101–104.

Arenas, R., Martínez-Catalán, J.R., Díaz García, F., 2004. Zona de Galicia-Trás-os-Montes. In: Vera, J.A. (Ed.), Geologia de España. Sociedad Geológica de España-Instituto Geológico y Minero de España, Madrid, España, pp. 133–165.

Barnett-Moore, N., Müller, R.D., Williams, S.E., Skogseid, J., Seton, M., 2018. A reconstruction of the north atlantic since the earliest Jurassic. Basin Res. 30, 160–185. https://doi.org/10.1111/bre.12214.

BeicipFranlab, Nalcor Energy Oil and Gas, Government of Newfoundland and Labrador, 2015. Offshore Newfoundland & Labrador Resource Assessment: Flemish Pass Area NL15_01EN. Nalcor Energy Oil and Gas, St. John's, NL, Canada.

BeicipFranlab, Nalcor Energy Oil and Gas, Government of Newfoundland and Labrador, 2016. Offshore Newfoundland & Labrador Resource Assessment Orphan Basin Area NL16-CFB01. Nalcor Energy Oil and Gas, St. John's, NL, Canada.

Bluck, B.J., Gibbons, W., Ingham, J.K., 1992. Terranes. In: Cope, J.C.W., Ingham, J.K., Rawson, P.F. (Eds.), Atlas of Palaeogeography and Lithofacies, Memoirs. Geological Society of London, pp. 1–4. https://doi.org/10.1144/GSL.MEM.1992.013.01.03.

Boillot, G., Auxietre, J.-L., Dunand, J.-P., Dupeuble, P.-A., Mauffret, A., 1979. The northwestern Iberian margin: a Cretaceous passive margin deformed during Eocene. In: Talwani, M., Hay, W., Ryan, W.B.F. (Eds.), Deep Drilling Results in the Atlantic Ocean: Continental Margins and Paleoenvironment, Maurice Ewing Series. American Geophysical Union, pp. 138–153. https://doi.org/10.1029/ME003p0138.

Boillot, G., Winterer, E.L., Meyer, A.W., Applegate, J., Baltuck, M., Bergen, J.A., Comas, M.C., Davies, T.A., Dunham, K., Evans, C.A., Girardeau, J., Goldberg, D., Haggerty, J.A., Jansa, L.E., Johnson, J.A., Kasahara, J., Loreau, J.-P., Luna, E., Moullade, M., Ogg, J.G., Sarti, M., Thurow, J., Williamson, M.A., 1987. Site 638. In: Littleton, R.M. (Ed.), Proceedings of the Ocean Drilling Program: Initial Reports, Proceedings of the Ocean Drilling Program. Ocean Drilling Program, . https://doi.org/10.2973/odp.proc.ir.103.109.1987.

Bonvalot, S., Balmino, G., Briais, A., Kuhn, M., Peyrefitte, A., Vales, N., Biancale, R., Gabalda, G., Moreaux, G., Reinquin, F., Sarrailh, M., 2012. World Gravity Map. BGI-CGMW-CNES-IRD, Paris, France.

Bouysse, P., coll, 2014. Geological Map of the World 1:35 M, third ed. CCGM-CGMW.

Boyden, J.A., Müller, R.D., Gurnis, M., Torsvik, T.H., Clark, J.A., Turner, M., Ivey-Law, H., Watson, R.J., Cannon, J.S., 2011. Next-generation plate-tectonic reconstructions using GPlates. In: Keller, G.R., Baru, C. (Eds.), Geoinformatics: Cyberinfrastructure for the Solid Earth Sciences. Cambridge University Press, Cambridge, pp. 95–114. https://doi.org/10.1017/CBO9780511976308.008.

Brune, S., Williams, S.E., Müller, R.D., 2018. Oblique rifting: the rule, not the exception. Solid Earth Discuss. 9, 1187–2018. https://doi.org/10.5194/se-2018-63.

Bulois, C., Pubellier, M., Chamot-Rooke, N., Watremez, L., 2018. From orogenic collapse to rifting: a case study of the northern Porcupine Basin, offshore Ireland. J. Struct. Geol. 114, 139–162. https://doi.org/10.1016/j.jsg.2018.06.021.

Burk, C.A., Drake, C.L. (Eds.), 1974. The Geology of Continental Margins. Springer-Science + Business Media, LLC. https://doi.org/10.1007/978-3-662-01141-6.

Calvès, G., Torvela, T., Huuse, M., Dinkleman, M.G., 2012. New evidence for the origin of the porcupine median Volcanic Ridge: early cretaceous volcanism in the Porcupine basin, atlantic margin of Ireland. Geochem. Geophys. Geosyst. 13, 1–18. https://doi.org/10.1029/2011GC003852.

Chen, C., Watremez, L., Prada, M., Minshull, T.A., Edwards, R., O'Reilly, B.M., Reston, T.J., Wagner, G., Kläschen, D., Shannon, P.M., 2018. From continental hyperextension to seafloor spreading: new insights on the Porcupine basin from wide-angle seismic data. J. Geophys. Res. Solid Earth. https://doi.org/10.1029/2018JB016375.

Chenin, P., Manatschal, G., Lavier, L.L., Erratt, D., 2015. Assessing the impact of orogenic inheritance on the architecture, timing and magmatic budget of the North Atlantic rift system: a mapping approach. J. Geol. Soc. Lond. 172, 711–720. https://doi.org/10.1144/jgs2014-139.

Chenin, P., Manatschal, G., Picazo, S., Müntener, O., Karner, G., Johnson, C., Ulrich, M., 2017. Influence of the architecture of magma-poor hyperextended rifted margins on orogens produced by the closure of narrow versus wide oceans. Geosphere 13, 559–576. https://doi.org/10.1130/GES01363.1.

Chew, D.M., 2009. Grampian orogeny. In: Holland, C.H., Sanders, I. (Eds.), The Geology of Ireland. Dunedin Academic Press, Edinburgh, United Kingdom, pp. 69–93.

Chew, D.M., Stillman, C.J., 2009. Late Caledonian orogeny and magmatism. In: Holland, C.H., Sanders, I. (Eds.), The Geology of Ireland. Dunedin Academic Press, Edinburgh, United Kingdom, pp. 143–173.

Chian, D., Reid, I.D., Jackson, H.R., 2001. Crustal structure beneath Orphan Basin and implications for nonvolcanic continental rifting. J. Geophys. Res. 106 (10) 923-10,940. https://doi.org/10.1029/2000JB900422.

Copestake, P., Ainsworth, N.R., Bailey, H.W., Gallagher, L.T., Gueinn, K., Hampton, M., Lavis, O., 1, M., Loy, T.1, Riley, L.A.4, Wright, T.D.1, 2018. A new standard lithostratigraphic framework for offshore Ireland. In: Atlantic Ireland 2018 Conference. Petroleum Affairs Division (PAD)-Petroleum Infrastructure Programme (PIP), Republic of Ireland.

Decarlis, A., Manatschal, G., Haupert, I., Masini, E., 2015. The tectono-stratigraphic evolution of distal, hyper-extended magma-poor conjugate rifted margins: examples from the Alpine Tethys and Newfoundland-Iberia. Mar. Pet. Geol. 68, 54–72. https://doi.org/10.1016/j.marpetgeo.2015.08.005.

Department of Mines and Energy, 2000. Sedimentary Basins and Hydrocarbon Potential of Newfoundland and Labrador (No. 2000– 01). Government of Newfoundland and Labrador, St. John's, Canada.

Divins, D.L., 2003. Total Sediment Thickness of the World's Oceans & Marginal Seas. NOAA National Geophysical Data Center, Boulder, CO.

Domeier, M., 2016. A plate tectonic scenario for the Iapetus and Rheic oceans. Gondwana Res. 36, 275–295. https://doi.org/10.1016/j.gr.2015.08.003.

Doré, A.G., Lundin, E.R., Jensen, L.N., Birkeland, Ø., Eliassen, P.E., Fichler, C., 1999. Principal tectonic events in the evolution of the northwest European Atlantic margin. In: Fleet, A.J., Boldy, S.A.R. (Eds.), Petroleum Geology of Northwest Europe: Proceedings of the 5th Petroleum Geology Conference. Geological Society, London, England, pp. 41–61. https://doi.org/10.1144/0050041.

Edwards, T., Jauer, C.D., Moir, P., Wielens, J.B. (Eds.), 2003. Tectonic Elements, Grand Banks of Newfoundland (East Coast Basin Atlas Series). East Coast Basin Atlas Series, . https://doi.org/10.4095/214599.

Enachescu, M., 1987. Tectonic and structural framework of the northeast Newfoundland continental margin. In: Beaumont, C., Tankard, A.J. (Eds.), Sedimentary Basins and Basin-Forming Mechanisms. Canadian Society of Petroleum Geologists, Calgary, Canada, pp. 117–146.

Enachescu, M., 2006. Structural setting and petroleum potential of the Orphan basin, offshore Newfoundland and labrador. CSEG Rec. 31, 5–13.

Enachescu, M., Kearsey, S., Hogg, J., Einarsson, P., Nader, S., Smee, J., 2004. Orphan basin, offshore Newfoundland, Canada: structural and tectonic framework, petroleum systems and exploration potential. In: SEG Int. Expo. 74th Annu. Meet. Expand. Abstr., vol. 23. pp. 382–385.

Enachescu, M., Kearsey, S., Hardy, V., Sibuet, J.-C., Hogg, J., Srivastava, S.P., Fagan, A., Thompson, T., Ferguson, R., 2005. Evolution and petroleum potential of Orphan basin, offshore Newfoundland, and its relation to the movement and rotation of flemish Cap based on plate kinematics of the north atlantic. In: Post, P.J., Rosen, N.C., Olson, D.L., Palmes, S.L., Lyons, K.T., Newton, G.B. (Eds.), Petroleum Systems of Divergent Continental Margin Basin, 25th Annual GCSSEPM Foundation—Bob F. Perkins Research Conference December 4–7. Houston, Texas, USA, pp. 75–131. https://doi.org/10.5724/gcs.05.25.0075.

Farias, P., Gallastegui, G., González Lodeiro, F., Marquínez, J., Martín Parra, L.M., Martínez-Catalán, J.R., de Pablo Maciá, J.G., Rodríguez Fernández, L.R., 1987. Aportaciones al conocimiento de la litoestratigrafía y estructura de Galicia Central. In: IX Reunião Sobre a Geologia Do Oeste Peninsular. Universidade do Porto, Porto, Portugal, pp. 411–431.

Fossen, H., 2010. Structural Geology, first ed. Cambridge University Press, Cambridge, United Kingdom.

Frizon De Lamotte, D., Fourdan, B., Leleu, S., Leparmentier, F., De Clarens, P., 2015. Style of rifting and the stages of Pangea breakup. Tectonics 34, 1009–1029. https://doi.

org/10.1002/2014TC003760.
Gagnevin, D., Haughton, P.D.W., Whiting, L., Saqab, M.M., 2017. Geological and geophysical evidence for a mafic igneous origin of the Porcupine Arch, offshore Ireland. J. Geol. Soc. Lond. https://doi.org/10.1144/jgs2017-041.
Galice, Groupe, 1979. The continental margin off Galicia and Portugal: acoustical stratigraphy, dredge stratigraphy, and structural evolution. In: Laughter, F.H., Fagerberg, E.M. (Eds.), Initial Reports of the Deep Sea Drilling Project. U.S. Government Printing Office, pp. 633–662. https://doi.org/10.2973/dsdp.proc.47-2.133.1979.
Gong, Z., Langereis, C.G., Mullender, T.A.T., 2008. The rotation of Iberia during the aptian and the opening of the Bay of Biscay. Earth Planet. Sci. Lett. 273, 80–93. https://doi.org/10.1016/j.epsl.2008.06.016.
Gouiza, M., Hall, J., Bertotti, G., 2015. Rifting and pre-rift lithosphere variability in the Orphan basin, Newfoundland margin, eastern Canada. Basin Res. 27, 367–386. https://doi.org/10.1111/bre.12078.
Gouiza, M., Hall, J., Welford, J.K., 2017. Tectono-stratigraphic evolution and crustal architecture of the Orphan basin during North Atlantic rifting. Int. J. Earth Sci. 106, 917–937. https://doi.org/10.1007/s00531-016-1341-0.
Harland, W.B., Gayer, R.A., 1972. The arctic caledonides and earlier oceans. Geol. Mag. 109, 289–314. https://doi.org/10.1017/S0016756800037717.
IOC, IHO, BODC, 2003. Centenary Edition of the GEBCO Digital Atlas. British Oceanographic Data Centre, Liverpool, United Kingdom.
Johnson, H., Ritchie, J.D., Gatliff, R.W., Williamson, J.P., Cavill, J., Bulat, J., 2001. Aspects of the structure of the Porcupine and Porcupine Seabight basins as revealed from gravity modelling of regional seismic transects. In: Shannon, P.M., Haughton, P.D.W., Corcoran, D.V. (Eds.), The Petroleum Exploration of Ireland's Offshore Basins, Special Publications. Geological Society of London, pp. 265–274. https://doi.org/10.1144/GSL.SP.2001.188.01.15.
Keen, C.E., Beaumont, C., 1990. Geodynamics of rifted continental margins. In: Keen, M.J., Williams, G.L. (Eds.), Geology of the Continental Margin of Eastern Canada. Geological Survey of Canada, Ottawa, Canada, pp. 393–472. https://doi.org/10.4095/132690.
Keen, M.J., Piper, D.J.W., 1990. Geological and historical perspective. In: Keen, M.J., Williams, G.L. (Eds.), Geology of the Continental Margin of Eastern Canada. Geological Survey of Canada, Ottawa, Canada, pp. 7–24. https://doi.org/10.4095/132690.
Keen, C.E., Stockmal, G.S., Welsink, H.J., Quinlan, G., Mudford, B., 1987. Deep crustal structure and evolution of the rifted margin northeast of Newfoundland: results from LITHOPROBE East. Can. J. Earth Sci. 24, 1537–1549. https://doi.org/10.1139/e87-150.
Keen, C.E., Dafoe, L.T., Dickie, K., 2014. A volcanic province near the Western termination of the Charlie-Gibbs Fracture Zone at the rifted margin, offshore northeast Newfoundland. Tectonics 33, 1133–1153. https://doi.org/10.1002/2014TC003547.
Keen, C.E., Dickie, K., Dafoe, L.T., 2018. Structural characteristics of the ocean-continent transition along the rifted continental margin, offshore central Labrador. Mar. Pet. Geol. 89, 443–463. https://doi.org/10.1016/j.marpetgeo.2017.10.012.
King, L.H., Fader, G.B., Poole, W.H., Wanless, R.K., 1985. Geological setting and age of the flemish Cap granodiorite, east of the Grand Banks of Newfoundland. Can. J. Earth Sci. 22, 1286–1298. https://doi.org/10.1139/e85-133.
Knott, S.D., Burchell, M.T., Jolley, E.J., Fraser, A.J., 1993. Mesozoic to Cenozoic plate reconstructions of the North Atlantic and hydrocarbon plays of the Atlantic margins. In: Parker, J.R. (Ed.), Petroleum Geology of Northwest Europe: Proceedings of the 4th Conference. Geological Society, London, United Kingdom, pp. 953–974. https://doi.org/10.1144/0040953.
Koning, T., Campbell, R.H., Hibbs, D.C., Leonhardt, G.W., 1988. An exploration case study of a world record deepwater wildcat well drilled in the Orphan basin, Newfoundland: blue H-28. In: Offshore Technology Conference, pp. 395–406. https://doi.org/10.4043/5661-MS.
Krawczyk, C.M., Reston, T.J., Beslier, M.-O., Boillot, G., 1996. Evidence for detachment tectonics on the Iberia Abyssal Plain rifted margin. In: Whitmarsh, R.B., Sawyer, D.S., Klaus, A., Masson, D.G. (Eds.), Proceedings of the Ocean Drilling Program - Scientific Results: Iberia Abyssal Plain. Ocean Drilling Program, pp. 603–615. https://doi.org/10.2973/odp.proc.sr.149.244.1996.
Kristoffersen, Y., 1978. Sea-floor spreading and the early opening of the North Atlantic. Earth Planet. Sci. Lett. 38, 273–290. https://doi.org/10.1016/0012-821X(78)90101-2.
Larsen, L.M., Heaman, L.M., Creaser, R.A., Duncan, R.A., Frei, R., Hutchison, M., 2009. Tectonomagmatic events during stretching and basin formation in the Labrador Sea and the Davis Strait: evidence from age and composition of Mesozoic to Palaeogene dyke swarms in West Greenland. J. Geol. Soc. Lond. 166, 999–1012. https://doi.org/10.1144/0016-76492009-038.
Lau, K.W.H., Watremez, L., Louden, K.E., Nedimović, M.R., 2015. Structure of thinned continental crust across the Orphan Basin from a dense wide-angle seismic profile and gravity data. Geophys. J. Int. 202, 1969–1992. https://doi.org/10.1093/gji/ggv261.
Lavier, L.L., Manatschal, G., 2006. A mechanism to thin the continental lithosphere at magma-poor margins. Nature 440, 324–328. https://doi.org/10.1038/nature04608.
Lilly, H.D., 1965. Submarine examination of the virgin rocks area, Grand Banks, Newfoundland: preliminary note. Bull. Geol. Soc. Am. 76, 131–132. https://doi.org/10.1130/0016-7606(1965)76[131:SEOTVR]2.0.CO;2.
Lister, G.S., Etheridge, M.A., Symonds, P.A., 1986. Detachment faulting and the evolution of passive continental margins. Geology 14, 246–250. https://doi.org/10.1130/0091-7613(1986)14<246:DFATEO>2.0.CO;2.
Louden, K.E., Tucholke, B.E., Oakey, G.N., 2004. Regional anomalies of sediment thickness, basement depth and isostatic crustal thickness in the North Atlantic Ocean. Earth Planet. Sci. Lett. 224, 193–211. https://doi.org/10.1016/j.epsl.2004.05.002.
Lundin, E.R., 2002. North Atlantic – Arctic: Overview of sea-floor spreading and rifting history. In: Eide, E. (Ed.), BATLAS – Mid Norway Plate Reconstructions Atlas with Global and Atlantic Perspectives. Geological Survey of Norway, pp. 40–47.
Lundin, E.R., Doré, A.G., 2011. Hyperextension, serpentinization, and weakening: a new paradigm for rifted margin compressional deformation. Geology 39, 347–350. https://doi.org/10.1130/G31499.1.
Martínez-Catalán, J.R., 1990. A non-cylindrical model for the northwest Iberian allochthonous terranes and their equivalents in the Hercynian belt of Western Europe. Tectonophysics 179, 253–272. https://doi.org/10.1016/0040-1951(90)90293-H.
Masson, D.G., Parson, L.M., 1983. Eocene deformation on the continental margin SW of the British Isles. J. Geol. Soc. Lond. 140, 913–920. https://doi.org/10.1144/gsjgs.140.6.0913.
Matte, P., 2001. The Variscan collage and orogeny (480-290 Ma) and the tectonic definition of the Armorica microplate: a review. Terra. Nova 13, 122–128. https://doi.org/10.1046/j.1365-3121.2001.00327.x.
Matthews, K.J., Maloney, K.T., Zahirovic, S., Williams, S.E., Seton, M., Müller, R.D., 2016. Global plate boundary evolution and kinematics since the late Paleozoic. Glob. Planet. Change 146, 226–250. https://doi.org/10.1016/j.gloplacha.2016.10.002.
Mauffret, A., Boillot, G., Auxietre, J.-L., Dunand, J.P., 1978. Évolution structurale de la marge continentale au Nord-Ouest de la péninsule ibérique. Bull. Soc. Géol. Fr. S7-XX 375–388. https://doi.org/10.2113/gssgfbull.S7-XX.4.375.
McKenzie, D., 1978. Some remarks on the development of sedimentary basins. Earth Planet. Sci. Lett. 40, 25–32. https://doi.org/10.1016/0012-821X(78)90071-7.
Mena, A., Francés, G., Pérez-Arlucea, M., Hanebuth, T.J.J., Bender, V.B., Nombela, M.A., 2018. Evolution of the Galicia Interior Basin over the last 60 ka: sedimentary processes and palaeoceanographic implications. J. Quat. Sci. https://doi.org/10.1002/jqs.3032.
Mitchum, R.M., Vail, P.R., Sangree, J.B., 1977. Seismic stratigraphy and global changes of sea level, Part 6: stratigraphic interpretation of seismic reflection patterns in depositional sequences. In: Payton, C.E. (Ed.), Seismic Stratigraphy — Applications to Hydrocarbon Exploration. Memoir. American Association of Petroleum Geologists, pp. 117–133.
Montadert, L., Winnock, E., Deltiel, J.R., Grau, G., 1974. Continental margins of Galicia-Portugal and Bay of Biscay. In: Burk, C.A., Drake, C.L. (Eds.), The Geology of Continental Margins. Springer-Verlag, pp. 323–342. https://doi.org/10.1007/978-3-662-01141-6.
Montadert, L., de Charpal, O., Roberts, D., Guennoc, P., Sibuet, J.-C., 1979. Northeast Atlantic passive continental margins: rifting and subsidence processes. In: Talwani, M., Hay, W., Ryan, W.B.F. (Eds.), Deep Drilling Results in the Atlantic Ocean: Continental Margin and Paleoenvironment, Maurice Ewing Series. American Geophysical Union, pp. 154–186. https://doi.org/10.1029/ME003p0154.
Montenat, C., Guery, F., Berthou, P.Y., 1988. Mesozoic evolution of the Lusitanian Basin: comparison with the adjacent margin. In: Mazzullo, E.K. (Ed.), Proceedings of the Ocean Drilling Program - Scientific Results: Galicia Margin. Ocean Drilling Program, pp. 757–775. https://doi.org/10.2973/odp.proc.sr.103.117.1988.
Morewood, N.C., Mackenzie, G.D., Shannon, P.M., O'Reilly, B.M., Readman, P.W., Makris, J., 2005. The crustal structure and regional development of the Irish Atlantic margin region. In: Doré, A.G., Vining, B.A. (Eds.), Petroleum Geology: North-West Europe and Global Perspectives—Proceedings of the 6th Petroleum Geology Conference. Geological Society of London, London, United Kingdom, pp. 1023–1033.
Müller, R.D., Seton, M., Zahirovic, S., Williams, S.E., Matthews, K.J., Wright, N.M., Shephard, G.E., Maloney, K.T., Barnett-Moore, N., Hosseinpour, M., Bower, D.J., Cannon, J., 2016. Ocean basin evolution and global-scale plate reorganization events since pangea breakup. Annu. Rev. Earth Planet Sci. 44, 107–138. https://doi.org/10.1146/annurev-earth-060115-012211.
Murillas, J., Mougenot, D., Boulot, G., Comas, M.C., Banda, E., Mauffret, A., 1990. Structure and evolution of the Galicia Interior basin (Atlantic western iberian continental margin). Tectonophysics 184. https://doi.org/10.1016/0040-1951(90)90445-E.
Murphy, J.B., Nance, R.D., 2008. The pangea conundrum. Geology 36, 703–706. https://doi.org/10.1130/G24966A.1.
Murphy, F.C., Anderson, T., Daly, J.S., Gallagher, V., Graham, J.R., Johnston, J.D., Kennan, P.S., Kennedy, M.J., Long, C.B., Morris, J.H., Keeffe, O., Parkes, M., Ryan, P.D., Sloan, R.J., Stillman, C.J., Todd, S.P., Wrafter, J.P., 1991. An appraisal of caledonian suspect terranes in Ireland. Ir. J. Earth Sci. 11, 11–41.
Murphy, J.B., Keppie, J.D., Nance, R.D., Dostal, J., 2010. Comparative evolution of the Iapetus and rheic oceans: a North America perspective. Gondwana Res. 17, 482–499. https://doi.org/10.1016/j.gr.2009.08.009.
Naliboff, J.B., Buiter, S.J.H., Péron-Pinvidic, G., Osmundsen, P.T., Tetreault, J., 2017. Complex fault interaction controls continental rifting. Nat. Commun. 8. https://doi.org/10.1038/s41467-017-00904-x.
Nance, R.D., Gutiérrez-Alonso, G., Keppie, J.D., Linnemann, U., Murphy, J.B., Quesada, C., Strachan, R.A., Woodcock, N.H., 2012. A brief history of the Rheic Ocean. Geosci. Front. 3, 125–135. https://doi.org/10.1016/j.gsf.2011.11.008.
Natural Resources Canada, 2017. Basin Database. http://basin.gdr.nrcan.gc.ca.
Naylor, D., Shannon, P.M., 2005. The structural framework of the Irish Atlantic Margin. In: Doré, A.G., Vining, B.A. (Eds.), Petroleum Geology: North-West Europe and Global Perspectives. Geological Society of London, London, United Kingdom, pp. 1009–1021. https://doi.org/10.1144/0061009.
Naylor, D., Shannon, P.M., Murphy, N., 2002. Porcupine-goban Region - a Standard Structural Nomenclature System.
Nirrengarten, M., Manatschal, G., Tugend, J., Kusznir, N.J., Sauter, D., 2018. Kinematic evolution of the southern North Atlantic: implications for the formation of hyperextended rift systems. Tectonics 37, 1–30. https://doi.org/10.1002/2017TC004495.
Norton, M.G., 2002. Tectonic Evolution of the Porcupine Basin (No. P00/8). Petroleum Affairs Division (PAD)-Petroleum Infrastructure Programme (PIP), Republic of Ireland.

Oakey, G.N., Stark, A., 1995. A Digital Compilation of Depth to Basement and Sediment Thickness for the North Atlantic and Adjacent Coastal Land Areas (No. Open File 3039). Geological Survey of Canada. https://doi.org/10.4095/203476.

O'Reilly, B.M., Hauser, F., Ravaut, C., Shannon, P.M., Readman, P.W., 2006. Crustal thinning, mantle exhumation and serpentinization in the Porcupine Basin, offshore Ireland: evidence from wide-angle seismic data. J. Geol. Soc. Lond. 163, 775–787. https://doi.org/10.1144/0016-76492005-079.

O'Sullivan, J.M., Jones, S.M., Hardy, R.J., 2010a. Comparative analysis of the porcupine median Volcanic Ridge with modern day pacific ocean seamounts – further evidence of an amagmatic mesozoic basin history for the south Porcupine basin, offshore Ireland. In: II Central and North Atlantic Conjugate Margins Conference. Método Directo, Lisbon, Portugal, pp. 216–219.

O'Sullivan, J.M., Jones, S.M., Hardy, R.J., 2010b. Geological Modelling of the Porcupine Median Ridge: Implications for the Hydrocarbon Prospectivity of North Atlantic Hyper-Extensional Basin and Margin Systems. Search Discov #10253.

Peace, A.L., Dempsey, E., Schiffer, C., Welford, J.K., McCaffrey, K., Imber, J., Phethean, J., 2018a. Evidence for basement reactivation during the opening of the Labrador sea from the makkovik province, labrador, Canada: insights from field data and numerical models. Geosciences 8, 308. https://doi.org/10.3390/geosciences8080308.

Peace, A.L., McCaffrey, K., Imber, J., van Hunen, J., Hobbs, R., Wilson, R., 2018b. The role of pre-existing structures during rifting, continental breakup and transform system development, offshore West Greenland. Basin Res. 30, 373–394. https://doi.org/10.1111/bre.12257.

Peace, A.L., Phethean, J.J.J., Franke, D., Foulger, G.R., Schiffer, C., Welford, J.K., McHone, G., Rocchi, S., Schnabel, M., Doré, A.G., 2019a. A review of Pangaea dispersal and Large Igneous Provinces – in search of a causative mechanism. Earth Sci. Rev. https://doi.org/10.1016/j.earscirev.2019.05.009.

Peace, A.L., Welford, J.K., Ball, P.J., Nirrengarten, M., 2019b. Deformable plate tectonic models of the southern North Atlantic. J. Geodyn. 128, 11–37. https://doi.org/10.1016/j.jog.2019.05.005.

Pereira, R., Alves, T.M., 2012. Tectono-stratigraphic signature of multiphased rifting on divergent margins (deep-offshore southwest Iberia, North Atlantic). Tectonics 31, 1–21. https://doi.org/10.1029/2011TC003001.

Pérez-Gussinyé, M., Reston, T.J., 2001. Rheological evolution during extension at nonvolcanic rifted margins: onset of serpentinization and development of detachments leading to continental breakup. J. Geophys. Res. Solid Earth 106, 3961–3975. https://doi.org/10.1029/2000JB900325.

Pérez-Gussinyé, M., Ranero, C.R., Reston, T.J., Sawyer, D.S., 2003. Mechanisms of extension at nonvolcanic margins: evidence from the Galicia interior basin, west of Iberia. J. Geophys. Res. Solid Earth 108, 1–19. https://doi.org/10.1029/2001JB000901.

Péron-Pinvidic, G., Manatschal, G., 2010. From microcontinents to extensional allochthons: witnesses of how continents rift and break apart? Pet. Geosci. 16, 189–197. https://doi.org/10.1144/1354-079309-903.

Péron-Pinvidic, G., Manatschal, G., Osmundsen, P.T., 2013. Structural comparison of archetypal Atlantic rifted margins: a review of observations and concepts. Mar. Pet. Geol. 43, 21–47. https://doi.org/10.1016/j.marpetgeo.2013.02.002.

Prada, M., Watremez, L., Chen, C., O'Reilly, B.M., Minshull, T.A., Reston, T.J., Shannon, P.M., Klaeschen, D., Wagner, G., Gaw, V., 2017. Crustal strain-dependent serpentinisation in the Porcupine Basin, offshore Ireland. Earth Planet. Sci. Lett. 474, 148–159. https://doi.org/10.1016/j.epsl.2017.06.040.

Readman, P.W., O'Reilly, B.M., Shannon, P.M., Naylor, D., 2005. The deep structure of the Porcupine Basin, offshore Ireland, from gravity and magnetic studies. In: Doré, A., Vining, B.A. (Eds.), Petroleum Geology: North-West Europe and Global Perspectives—Proceedings of the 6th Petroleum Geology Conference. Geological Society of London, London, United Kingdom, pp. 1047–1056.

Réhault, J.-P., Mauffret, A., 1979. Relationships between tectonics and sedimentation around the northwestern iberian margin. In: Laughter, F.H., Fagerberg, E.M. (Eds.), Initial Reports of the Deep Sea Drilling Project. U.S. Government Printing Office, pp. 663–681. https://doi.org/10.2973/dsdp.proc.47-2.134.1979.

Reston, T.J., 2007. Extension discrepancy of North Atlantic nonvolcanic rifted margins: depth-dependent stretching or unrecognized faulting? Geology 35, 367–370. https://doi.org/10.1130/G23213A.1.

Reston, T.J., 2009. The structure, evolution and symmetry of the magma-poor rifted margins of the North and Central Atlantic: a synthesis. Tectonophysics 6–27. https://doi.org/10.1016/j.tecto.2008.09.002.

Reston, T.J., Pennell, J., Stubenrauch, A., Walker, I., Pérez-Gussinyé, M., 2001. Detachment faulting, mantle serpentinization, and serpentinite-mud, volcanism beneath the Porcupine Basin, southwest of Ireland. Geology 29, 587–590. https://doi.org/10.1130/0091-7613(2001)029<0587:DFMSAS>2.0.CO;2.

Reston, T.J., Gaw, V., Pennell, J., Kläschen, D., Stubenrauch, A., Walker, I., 2004. Extreme crustal thinning in the south Porcupine Basin and the nature of the Porcupine Median High: implications for the formation of non-volcanic rifted margins. J. Geol. Soc. Lond. 161, 783–798. https://doi.org/10.1144/0016-764903-036.

Roberts, D.G., Thompson, M., Mitchener, B., Hossack, J., Carmichael, S., Bjørnseth, H., 1999. Palaeozoic to Tertiary rift and basin dynamics: mid-Norway to the Bay of Biscay − a new context for hydrocarbon prospectivity in the deep water frontier Palaeozoic to Tertiary rift and basin dynamics: mid-Norway to the Bay of Biscay - a new context for. In: Fleet, A.J., Boldy, S.A. (Eds.), Petroleum Geology of Northwest Europe: Proceedings of the 5th Conference. Geological Society, London, United Kingdom, pp. 7–40. https://doi.org/10.1144/0050007.

Sclater, J.G., Christie, P.A.F., 1980. Continental stretching: an explanation of the post-mid-cretaceous subsidence of the central north sea basin. J. Geophys. Res. Solid Earth 85, 3711–3739. https://doi.org/10.1029/JB085iB07p03711.

Seton, M., Müller, R.D., Zahirovic, S., Gaina, C., Torsvik, T.H., Shephard, G.E., Talsma, A., Gurnis, M., Turner, M., Maus, S., Chandler, M., 2012. Global continental and ocean basin reconstructions since 200Ma. Earth Sci. Rev. 113, 212–270. https://doi.org/10.1016/j.earscirev.2012.03.002.

Shannon, P.M., Naylor, D., 1998. An assessment of Irish offshore basins and petroleum plays. J. Pet. Geol. 21, 125–152. https://doi.org/10.1111/j.1747-5457.1998.tb00651.x.

Shannon, P.M., Jacob, A.W.B., O'Reilly, B.M., Hauser, F., Readman, P.W., Makris, J., 1999. Structural setting, geological development and basin modelling in the Rockall Trough. In: Fleet, A.J., Boldy, S.A.R. (Eds.), Petroleum Geology of Northwest Europe: Proceedings of the 5th Petroleum Geology Conference. Geological Society, London, England, pp. 421–431. https://doi.org/10.1144/0050421.

Shannon, P.M., Corcoran, D.V., Haughton, Peter D.W., 2001. The petroleum exploration of Ireland's offshore basins: introduction. In: Shannon, P.M., Haughton, P.D.W., Corcoran, D.V (Eds.), The Petroleum Exploration of Ireland's Offshore Basins, Special Publications. Geological Society of London, pp. 1–8. https://doi.org/10.1144/GSL.SP.2001.188.01.01.

Shannon, P.M., McDonnell, A., Bailey, W.R., 2007. The evolution of the Porcupine and Rockall basins, offshore Ireland: the geological template for carbonate mound development. Int. J. Earth Sci. 96, 21–35. https://doi.org/10.1007/s00531-006-0081-y.

Sheriff, R.E., Geldart, L.P., 1995. Exploration Seismology, second ed. Cambridge University Press, United States of America.

Sibuet, J.-C., Collette, B.J., 1991. Triple junctions of Bay of Biscay and North Atlantic: new constraints on the kinematic evolution. Geology 19, 522–525. https://doi.org/10.1130/0091-7613(1991)019<0522:TJOBOB>2.3.CO;2.

Sibuet, J.-C., Ryan, W.B.F., Arthur, M.A., Barnes, R.O., Habib, D., Iaccarino, S., Johnson, D., Lopatin, B., Maldonado, A., Moore, D.G., Morgan, G.E., Réhault, J.-P., Sigal, J., Williams, C.A., 1979. Site 398. In: Laughter, F.H., Fagerberg, E.M. (Eds.), Initial Reports of the Deep Sea Drilling Project. U.S. Government Printing Office, pp. 25–233. https://doi.org/10.2973/dsdp.proc.47-2.102.1979.

Sibuet, J.-C., Srivastava, S.P., Spakman, W., 2004. Pyrenean orogeny and plate kinematics. J. Geophys. Res. Solid Earth 109, 1–18. https://doi.org/10.1029/2003JB002514.

Sibuet, J.-C., Srivastava, S.P., Enachescu, M., Karner, G.D., 2007. Early cretaceous motion of flemish Cap with respect to north America: implications on the formation of Orphan basin and SE flemish Cap Galicia Bank conjugate margins. In: Karner, G.D., Manatschal, G., Pinheiro, L.M. (Eds.), Imaging, Mapping and Modelling Continental Lithosphere Extension and Breakup. Geological Society, London, England, pp. 63–76. https://doi.org/10.1144/SP282.4.

Skogseid, J., 2010. The Orphan Basin – a key to understanding the kinematic linkage between North and NE Atlantic Mesozoic rifting. In: Dos Reis, R.P., Pimentel, N. (Eds.), II Central and North Atlantic Conjugate Margins Conference. Open Journal Systems 2.3.8.0, Lisbon, Portugal, pp. 13–23.

Skogseid, J., Barnwell, A., Aarseth, E.S., Alsgaard, P.C., Briseid, H.C., Zwach, C., 2004. Orphan basin: multiple 'Failed' rifting during early opening of the north Atlantic. Eos Trans. Am. Geophys. Union.

Smee, J., Nader, S., Einarsson, P., Hached, R., Enachescu, M., 2003. Orphan basin, offshore Newfoundland: new seismic data and hydrocarbon plays for a dormant frontier basin. In: Joint CSPG/CSEG National Convention, Conference, pp. 7.

Srivastava, S.P., Verhoef, J., 1992. Evolution of Mesozoic sedimentary basins around the North Central Atlantic: a preliminary plate kinematic solution. In: Parnell, J. (Ed.), Basins on the Atlantic Seaboard: Petroleum Geology, Sedimentology and Basin Evolution, Special Publications. Geological Society, London, England, pp. 397–420. https://doi.org/10.1144/GSL.SP.1992.062.01.30.

Srivastava, S.P., Verhoef, J., Macnab, R., 1988. Results from a detailed aeromagnetic survey across the northeast Newfoundland margin, Part II: early opening of the north Atlantic between the British isles and Newfoundland. Mar. Pet. Geol. 5, 324–337. https://doi.org/10.1016/0264-8172(88)90026-8.

Srivastava, S.P., Roest, W.R., Kovacs, L.C., Oakey, G.N., Lévesque, S., Verhoef, J., Macnab, R., 1990. Motion of Iberia since the late Jurassic: results from detailed aeromagnetic measurements in the Newfoundland Basin. Tectonophysics 184, 229–260. https://doi.org/10.1016/0040-1951(90)90442-B.

Sutra, E., Manatschal, G., Mohn, G., Unternehr, P., 2013. Quantification and restoration of extensional deformation along the Western Iberia and Newfoundland rifted margins. Geochem. Geophys. Geosyst. 14, 2575–2597. https://doi.org/10.1002/ggge.20135.

Tate, M.P., 1992. The Clare Lineament: a relic transform fault west of Ireland. In: Parnell, J. (Ed.), Basins on the Atlantic Seaboard: Petroleum Geology, Sedimentology, and Basin Evolution, Special Publication. Geological Society, London, United Kingdom, pp. 375–384. https://doi.org/10.1144/GSL.SP.1992.062.01.28.

Tate, M.P., Dobson, M.R., 1988. Syn- and post-rift igneous activity in the Porcupine Seabight Basin and adjacent continental margin W of Ireland. In: Morton, A.C., Parson, L.M. (Eds.), Early Tertiary Volcanism and the Opening of the NE Atlantic. Special Publication. Geological Society of London, London, pp. 309–334. https://doi.org/10.1144/GSL.SP.1988.039.01.28.

Thomas, W.A., 2006. Tectonic inheritance at a continental margin. GSA Today 16, 4–11. https://doi.org/10.1130/1052-5173(2006)016<4.

Thompson, T., 2003. Preliminary findings on basin architecture , segmentation and inversion on a passive margin offshore Newfoundland. In: CSEG Annual Conference. Canadian Society of Exploration Geophysicists, Canada.

Tugend, J., Manatschal, G., Kusznir, N.J., Masini, E., Mohn, G., Thinon, I., 2014. Formation and deformation of hyperextended rift systems: insights from rift domain mapping in the Bay of Biscay-Pyrenees. Tectonics 33, 1239–1276. https://doi.org/10.1002/2014TC003529.

Tyrrell, S., Haughton, P.D.W., Daly, J.S., 2007. Drainage reorganization during breakup of Pangea revealed by in-situ Pb isotopic analysis of detrital K-feldspar. Geology 35, 971–974. https://doi.org/10.1130/G4123A.1.

van der Pluijm, B.A., Marshak, S., 2004. Earth Structure, second ed. W. W. Norton &

Company, Inc., United States of America.
Vissers, R.L.M., Meijer, P.T., 2012. Mesozoic rotation of Iberia: subduction in the pyrenees? Earth Sci. Rev. 110, 93–110. https://doi.org/10.1016/j.earscirev.2011.11.001.
Watremez, L., Prada, M., Minshull, T.A., O'Reilly, B.M., Chen, C., Reston, T.J., Shannon, P.M., Wagner, G., Gaw, V., Kläschen, D., Edwards, R., Lebedev, S., 2016. Deep structure of the Porcupine Basin from wide-angle seismic data. In: Petroleum Geology Conference Series. Geological Society, London, United Kingdom, pp. 199–209. https://doi.org/10.1144/PGC8.26.
Welford, J.K., Hall, J., Sibuet, J.-C., Srivastava, S.P., 2010. Structure across the northeastern margin of Flemish Cap, offshore Newfoundland from Erable multichannel seismic reflection profiles: evidence for a transtensional rifting environment. Geophys. J. Int. 183, 572–586. https://doi.org/10.1111/j.1365-246X.2010.04779.x.
Welford, J.K., Shannon, P.M., O'Reilly, B.M., Hall, J., 2012. Comparison of lithosphere structure across the Orphan Basin–Flemish Cap and Irish Atlantic conjugate continental margins from constrained 3D gravity inversions. J. Geol. Soc. Lond. 169, 405–420. https://doi.org/10.1144/0016-76492011-114.
Williams, H., 1979. Appalachian orogen in Canada. Can. J. Earth Sci. 16, 792–807. https://doi.org/10.1139/e79-070.
Williams, H., Dehler, S.A., Grant, A.C., Oakey, G.N., 1999. Tectonics of Atlantic Canada. Geosci. Canada 26, 51–70.
Wilson, J.T., 1966. Did the Atlantic close and then re-open? Nature 211, 676–681. https://doi.org/10.1038/211676a0.
Wilson, R.C.L., Hiscott, R.N., Willis, M.G., Gradstein, F.M., 1989. The Lusitanian Basin of west-central Portugal; Mesozoic and Tertiary tectonic, stratigraphic, and subsidence history. In: Tankard, A.J., Balkwill, H.R. (Eds.), Extensional Tectonics and Stratigraphy of the North Atlantic Margins. Memoir. American Association of Petroleum Geologists, pp. 341–361.
Woodward, N.B., Boyer, S.E., Suppe, J., 1989. Balanced Geological Cross-Sections: an Essential Technique in Geological Research and Exploration, Short Course in Geology. American Geophysical Union, Washington, D. C. https://doi.org/10.1029/SC006.
Ziegler, P.A., 1982. Geological Atlas of Western and Central Europe, first ed. Shell Internationale Petroleum Maatschappij B.V., The Hague, The Netherlands.
Ziegler, P.A., 1988. Evolution of the Arctic-North Atlantic and the Western Tethys, AAPG Memoir. American Association of Petroleum Geologists.